Performance Analysis of RIS-Aided Index Modulation with Greedy Detection over Rician Fading Channels

Aritra Basu, Soumya P. Dash, *Member, IEEE*, Aryan Kaushik, *Member, IEEE*, Debasish Ghose, *Senior Member, IEEE*, Marco Di Renzo, *Fellow, IEEE*, and Yonina C. Eldar, *Fellow, IEEE*

***Abstract*—Index modulation (IM) schemes for reconfigurable intelligent surfaces (RIS)-assisted systems are envisioned as promising technologies for fifth-generation-advanced and sixth-generation (6G) wireless communication systems to enhance various system capabilities such as coverage area and network capacity. In this paper, we consider a receive diversity RIS-assisted wireless communication system employing IM schemes, namely, space-shift keying (SSK) with binary modulation and spatial modulation (SM) with M-ary modulation for data transmission. The RIS lies in close proximity to the transmitter, and the transmitted data is subjected to a fading environment with a prominent line-of-sight component statistically modeled by a Rician distribution. A receiver structure based on a greedy detection rule is employed to select the receive diversity branch with the highest received signal energy for demodulation. The performance of the considered system is evaluated by obtaining a series-form expression for the probability of erroneous index detection (PED) of the considered target antenna using a characteristic function approach. In addition, closed-form and asymptotic expressions at high and low signal-to-noise ratios (SNRs) for the bit error rate (BER) of the SSK-based system, and the SM-based system employing M-ary phase-shift keying and M-ary quadrature amplitude modulation schemes are derived. The dependencies of the system performance on various parameters are corroborated via numerical results. The asymptotic expressions and results of PED and BER at high and low SNR values lead to the observation of a performance saturation and the presence of an SNR value as a point of inflection, which is attributed to the greedy detector.**

***Index Terms*—Index modulation, reconfigurable intelligent surface, rician fading, space-shift keying, spatial modulation.**

I. Introduction

Fifth-generation (5G) wireless communication systems promise to achieve high spectrum efficiency and energy efficiency that has led to a new vision of mobile communications, broadly catering to use cases with requirements of enhanced mobile broadband, ultra-reliability, and low-latency for massive machine-type communications [1]. Since it becomes very challenging for a single enabling technology to cater to all these demands, researchers, in a bid to make the communication systems future-ready, have started to explore advanced 5G and 6th-generation (6G) envisioned technologies. New user requirements, applications, use cases, and networking trends are expected to thrive, which will necessitate new communication paradigm shifts, especially at the physical layer [2], [3]. Within this context for the development of next-generation wireless communication technologies [4]–[6], there has been increasing interest in controlling the properties of the physical channel/medium, which has led to the popularity of reconfigurable intelligent surfaces (RIS) [7]–[9]. Furthermore, the application of other new technologies, such as index modulation (IM) to RIS-assisted systems, has piqued the interest of researchers over recent years.

A. Literature Review

RIS, consisting of reconfigurable scattering elements, influences the wireless medium/channel in which it is placed. The ease of deployment of thin artificial films of RIS results in a reduction in implementation cost and system complexity [10]–[12]. Moreover, RIS technology, considered a nearly passive form of a relay [13]–[17], does not require a dedicated energy source to cater to different RF processing, encoding, decoding, or re-transmission, and are thus, efficient over existing multiple-input multiple-output (MIMO), beamforming, amplify-and-forward relaying, and backscatter communication paradigms [18]–[20]. Furthermore, the reflection characteristics of an RIS may be controlled by software; hence an RIS is also referred to as a software-defined surface and can be employed as a substitute for traditional beamforming techniques [21]. RIS-based system improvements in the form of a number-modulation scheme over symbiotic active/passive communications are proposed by the authors of [22]. Additionally, the investigation of the ergodic capacity of an RIS-assisted multi-user multiple-input single-output system with practical statistical channel state information (CSI) is discussed by the authors of [23]. Instantaneous CSI alternatives using a low-complexity algorithm via the two-timescale transmission protocol are proposed by the authors of [24] and incorporation of RIS in 6G terahertz communication using deep reinforcement method is analyzed in [25].

Another vital aspect of beyond 5G systems is the use of IM [26], [27], which specifies a type of modulation technique relying on some form of activation states for information embedding, carried out in different domains like space, time, and frequency slots, or even a combination of them. The

The work of A. Kaushik has been supported by the UKRI Higher Education Innovation Fund project "Net Zero and Sustainable 6G: Communications, Sensing and Computing".

The work of M. Di Renzo was supported in part by the European Commission through the H2020 ARIADNE project under grant agreement number 871464 and through the H2020 RISE-6G project under grant agreement number 101017011, and by the Agence Nationale de la Recherche (France 2030, ANR PEPR Future Networks, grant NF-Founds 22-PEFT-0010).

A. Basu and S. P. Dash are with the School of Electrical Sciences, Indian Institute of Technology Bhubaneswar, Argul, Khordha, 752050 India e-mail: (21ec06008@iitbbs.ac.in, soumyapdashiitbbs@gmail.com).

A. Kaushik is with the School of Engineering and Informatics, University of Sussex, Brighton, UK, e-mail: aryan.kaushik@sussex.ac.uk.

D. Ghose is with the School of Economics, Innovation, and Technology, Kristiania University College, Bergen, Norway 5022, e-mail: debasish.ghose@kristiania.no.

M. Di Renzo is with Université Paris-Saclay, CNRS, CentraleSupélec, Laboratoire des Signaux et Systèmes, 3 Rue Joliot-Curie, 91192 Gif-sur-Yvette, France. (marco.di-renzo@universite-paris-saclay.fr)

Y. C. Eldar is with Weizmann Institute of Science, Rehovot 7610001, Israel, e-mail: yonina.eldar@weizmann.ac.il.

basic principle of IM is to separate the information bits into index and constellation bits. The former specifies the portion of the active radio resources (antennas and sub-carriers), and the latter bits are used for mapping conventional constellation symbols to be carried by the active resources [28], [29]. In this category, space-shift keying (SSK) and spatial modulation (SM) exploit the spatial-constellation diagram for data modulation, resulting in a low-complexity modulation for multiple-antenna systems, and they outperform conventional modulation schemes in terms of spectral efficiency [30]–[33]. Though the basic principle behind index-modulated SSK or SM schemes is similar in terms of data modulation, SM-based index-modulated systems are more complex due to the additional requirement of a modulation system/scheme in the form of amplitude/phase modulation. RIS-assisted SSK-based systems can be further improved in terms of error and throughput by incorporating passive beamforming and Alamouti space-time block coding as studied in [34].

Several studies have been proposed in the literature for RIS-assisted IM-based system models. The authors of [18] proposed three IM-based communication system architectures: IM for the source transmit antennas; IM for the destination receive antennas; and IM for the RIS that applies reflection modulation-based beam patterns. Also, the authors analyzed the system in terms of pairwise error probability. A hybrid concept employing IM and metasurface modulation was studied in [11] to improve the system performance. An RIS grouping-based IM scheme to enhance the spectral efficiency and improve the bit error rate was presented in [35]. The authors of [36] introduced the concept of reflection modulation, whereas the authors of [37] proposed a non-coherent receiver for a reflection modulation-based RIS-assisted system to further reduce the hardware complexity. The performance loss associated with an RIS-assisted SSK modulated system with a blind receiver was examined in [38]. The authors of [18] and [17] considered SSK and SM schemes for a receive diversity RIS-assisted communication system wherein they proposed a greedy detector for detecting the diversity branch with maximum received energy and utilized the same for data demodulation. With this system model, the authors of [18] obtained upper bounds on the system performance, and the authors of [17] derived closed-form expressions for the same performance metrics.

B. Contributions

RIS systems are generally utilized owing to the lack of a line of sight (LoS) communication path between the transmitter and the receiver end, thus resulting in an LoS path being present between the transmitter-RIS link and the RIS-receiver link. However, most previously carried out works for IM-based RIS-assisted systems do not consider the scenario where the channel gains follow Rician fading [39]–[41], thus failing to model communication scenarios that possess significant or dominant LoS components. We consider an SSK/SM-based RIS-assisted wireless system in which the envelopes of the channel gains follow the Rician distribution, thus being able to properly model the scenario between the RIS and the receiver that possesses a dominant LoS path. The SSK system is considered for binary modulation schemes, and the SM system is considered for the transmission of M-ary modulated data symbols. Further motivated by the studies in [17], [18], we employ a greedy detector at the receiver and study the system performance in terms of the probability of erroneous detection (PED) of the corresponding antenna of interest. The contributions of the work are summarized as follows:

- A receive diversity wireless communication system subject to Rician fading channels is considered wherein the transmitter, lying in close proximity to the RIS, employs an IM based on SSK or M-ary phase-shift keying (M-PSK)/M-ary quadrature amplitude modulation (QAM) constellation-based SM scheme.
- A greedy detector structure [17] is employed for the considered RIS-assisted wireless system, which relies on the maximum energy of the received signals at the receive diversity branches to be selected for demodulation without the need for channel estimation.
- An analytical framework based on a characteristic function (c.f.) approach is proposed to obtain exact closed-form expressions for the PED of the target receive diversity antenna in RIS-assisted SSK and SM systems.
- Expressions for the symbol error probability (SEP) of both systems are derived, based on which the asymptotic expressions at high and low signal-to-noise ratios (SNR) provide insight into the dependency of the performance of the system on various system parameters.
- Numerical results are presented to study the effect of the system parameters on the PED and the bit error rate (BER), which showcase the dependency of the LoS component on these metrics.

The rest of the paper is organized as follows. The model of the SSK-based and SM-based RIS-assisted systems and the greedy detector are presented in Section II. The analytical frameworks to derive closed-form and asymptotic expressions of the PED of the target receive diversity antenna for the considered RIS-assisted IM-based systems are given in Sections III and IV. The corresponding derivation to obtain the exact and asymptotic expressions of the SEP of the system is provided in Section V. Section VI presents numerical results corroborating the analytical studies, followed by concluding remarks provided in Section VII.

II. System Model

An RIS-assisted wireless communication system is considered where the RIS consists of N reconfigurable scattering elements and is placed in close proximity to the transmitter, similar to the concept of an RIS access point (AP) in which the RIS can be considered as a part of the transmitter [18]. The receiver, lying in the far field of the RIS to model conventional communication scenarios, comprises of $N_{R\text{x}}$ diversity branches which obtain the signal from the transmitter via the reflections from the RIS elements. The wireless fading channel between the i-th reconfigurable element of the RIS and the w-th receive diversity branch is modeled as a complex multiplicative gain coefficient and is denoted by

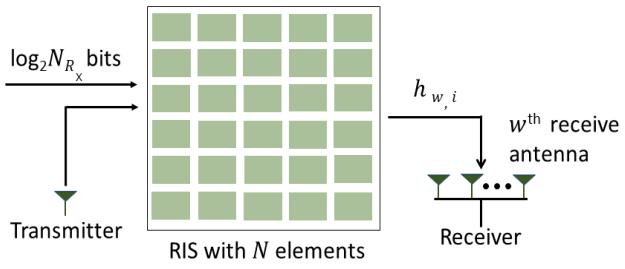

Fig. 1. System model for the implementation of the RIS-assisted SSK scheme.

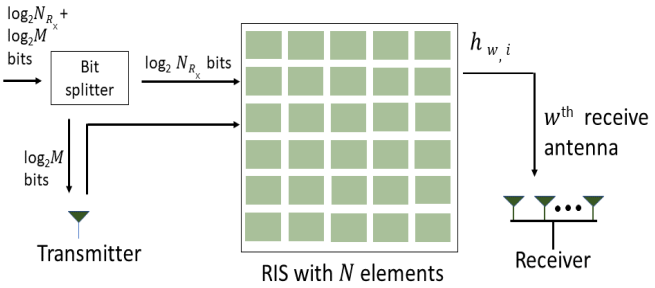

Fig. 2. System model for the implementation of the RIS-assisted SM schemes.

$h_{w,i} = \beta_{w,i} \exp\{-\jmath\psi_{w,i}\}$, where $\jmath = \sqrt{-1}$, $w = 1, \ldots, N_{R_\text{X}}$, and $i = 1, \ldots, N$. The transmitter employs (i) SSK or (ii) M-ary QAM/M-PSK constellation-based SM for IM, and the receiver employs a greedy detector to select the receive diversity branch for optimal performance. Furthermore, it is assumed that all the channels between the RIS and the receiver are statistically independent and identically distributed (i.i.d.) and that the transmitter has perfect knowledge of the information of the channel states [17], [18]. We assume that the envelopes of the i.i.d. channel gains follow the Rician distribution, implying that each complex channel gain $h_{w,i}$ follows a non-zero mean complex Gaussian distribution, i.e., $h_{w,i} \sim \mathcal{CN}\left(\mu, \sigma_h^2\right)$, where $\mathbf{E}\left[h_{w,i}\right] = \mu$ ($\mathbf{E}\left[\cdot\right]$ denotes the expectation operator), $\mathbf{E}\left[\left(h_{w,i} - \mu\right)^2\right] = \sigma_h^2$, and the Rician factor of the system is denoted as $k = |\mu|^2/\sigma_h^2$.

A. RIS-Assisted SSK System

The RIS-SSK system, as shown in Fig. 1, aims at maximizing the instantaneous received SNR at a target receive diversity branch by intelligently adjusting the phase shifts of the RIS elements with respect to the channel phases before reflecting the transmitted signal towards the receiver. The receiver performs the elementary task of determining the index of the target diversity branch by utilizing the received $\log_2 N_{R_\text{X}}$ bits.

Considering the energy of the transmitted symbol to be $\sqrt{E_s}$, the received signal at the w-th diversity branch can be expressed as

$$z_w = \sqrt{E_s}\left[\sum_{i=1}^{N} h_{w,i} \exp\{\jmath\phi_i\}\right] + n_w\,,\; w = 1, \ldots, N_{R_\text{X}}\,, \tag{1}$$

where ϕ_i denotes the phase shift introduced by the i-th RIS element and n_w is the additive noise at the w-th receive diversity branch, which follows a zero-mean complex Gaussian distribution, implying that $n_w \sim \mathcal{CN}\left(0, N_0\right)$ with $\mathbf{E}\left[|n_w|^2\right] = N_0$. Furthermore, the noise n_w is statistically independent of $h_{w,i}$ and $\phi_i \in i = \{1, \ldots, N\}$.

From (1), the instantaneous received SNR at the w-th receive diversity branch is given by

$$\gamma_w = \frac{\left|\sum_{i=1}^{N} \beta_{w,i} \exp\{\jmath\left(\phi_i - \psi_{w,i}\right)\}\right|^2 E_s}{N_0}\,,\; w = 1, \ldots, N_{R_\text{X}}\,, \tag{2}$$

which can be maximized by adjusting the phases of the RIS elements as $\phi_i = \psi_{w,i}$. This results in the expression of the maximum SNR at the selected w-th receive diversity branch, given by

$$\gamma_{w,max} = \frac{\left|\sum_{i=1}^{N} \beta_{w,i}\right|^2 E_s}{N_0}\,,\; w = 1, \ldots, N_{R_\text{X}}\,. \tag{3}$$

B. RIS-Assisted SM System

The RIS-SM system, shown in Fig. 2, aims to improve the system spectral efficiency and to maximize the instantaneous SNR at the target receive diversity branch. Thus, apart from the selection of the phase shifts of the RIS elements, the transmitter employs an M-ary QAM/M-PSK modulation scheme for data transmission. Thus, as in the case of the RIS-assisted SSK system, the first set of $\log_2 N_{R_\text{X}}$ bits is used for the determination of the index of the target antenna as well as to adjust the phases to maximize the instantaneous received SNR at the target antenna index, and the second set of $\log_2 M$ bits is utilized to generate the M-ary modulated symbol via an RF source. The received signal at the w-th diversity branch is then expressed as

$$z_w = \left[\sum_{i=1}^{N} h_{w,i} \exp\{\jmath\phi_i\}\right] v_\zeta + n_w\,,\; w = 1, \ldots, N_{R_\text{X}}\,, \tag{4}$$

where v_ζ is the data symbol belonging to the M-ary QAM/M-PSK constellation, $\mathbf{E}\left[|v_\zeta|^2\right] = E_s$, and n_w is the additive noise with $n_w \sim \mathcal{CN}\left(0, N_0\right)$.

C. Greedy Detector

The receivers for the RIS-SSK and RIS-SM systems employ a greedy detector [17], [18] to obtain the index of the receive diversity branch associated with the highest instantaneous received energy without the need for CSI at the receiver end. Thus, the index w of the target antenna for the considered non-coherent receiver is selected by using the decision rule, given as

$$\hat{w} = \arg\max_{w} |z_w|^2\,. \tag{5}$$

Thus, the greedy detector chooses the *target antenna* according to the maximum instantaneous SNR at the diversity branches. In the following sections, we derive expressions for the PED of the target antenna of RIS-assisted SSK and SM systems.

III. PED Analysis of the RIS-Assisted SSK System

In this section, we derive a series-form expression for the probability of erroneous detection of the receive antenna index detection for the RIS-SSK scheme using the greedy detector.

A. Pairwise PED Analysis

Let w and $\hat{w}$ be the indices of the target and some other non-target antennas, where the term *target antenna* is used for the receive diversity branch leading to the maximum received energy. Using (1), the expression for the pairwise PED (PPED) of the target antenna is computed as

$$\Pr\left\{|z_{w_{ssk}}|^2 < |z_{\hat{w}_{ssk}}|^2\right\} = \Pr\left\{\left|\sqrt{E_s}\sum_{i=1}^{N} h_{w,i}e^{\jmath\phi_i} + n_w\right| < \left|\sqrt{E_s}\sum_{i=1}^{N} h_{\hat{w},i}e^{\jmath\phi_i} + n_{\hat{w}}\right|\right\}. \quad (6)$$

We wish to maximize the signal energy for the target antenna, which can be expressed as an optimization problem by substituting (1) in (6) as

$$\min_{\{\phi_i\}_{i=1}^N} \Pr\left\{\left|\sum_{i=1}^{N}\beta_{\hat{w},i}\exp\left\{\jmath\left(\phi_i - \psi_{\hat{w}_i,i}\right)\right\}\right|^2 > \left|\sum_{i=1}^{N}\beta_{w,i}\exp\left\{\jmath\left(\phi_i - \psi_{w_i,i}\right)\right\}\right|^2\right\}. \quad (7)$$

It can be observed that (7) is minimized by choosing the values of the phase shifts of the reflecting elements constituting the RIS as $\phi_i = \psi_{w,i}$ for $i = 1, \ldots, N$, resulting in the optimization problem

$$\min_{\{\phi_i\}_{i=1}^N} \Pr\left\{\left|\sum_{i=1}^{N}\beta_{\hat{w},i}\exp\left\{\jmath\left(\phi_i - \psi_{\hat{w}_i,i}\right)\right\}\right|^2 > \left|\sum_{i=1}^{N}\beta_{w,i}\right|^2\right\}, \quad (8)$$

whose corresponding PPED is given by

$$\Pr\left\{|z_{w_{ssk}}|^2 < |z_{\hat{w}_{ssk}}|^2\right\} = \Pr\left\{\left|\sqrt{E_s}\sum_{i=1}^{N}\beta_{w,i} + n_w\right|^2 < \left|\sqrt{E_s}\sum_{i=1}^{N}\beta_{\hat{w},i}\exp\left\{\jmath\left(\psi_{w,i} - \psi_{\hat{w},i}\right)\right\} + n_{\hat{w}}\right|^2\right\}. \quad (9)$$

From the statistics of the complex channel gains, $\beta_{w,1}, \ldots, \beta_{w,N}$ and $\beta_{\hat{w},1}, \ldots, \beta_{\hat{w},N}$ are i.i.d. random variables, each following a Rician distribution. Moreover, $\psi_{w,1}, \ldots, \psi_{w,N}$ and $\psi_{\hat{w},1}, \ldots, \psi_{\hat{w},N}$ are i.i.d. random variables. Thus, utilizing the central limit theorem, the statistical distribution of (9) is given by [42], as follows:

$$\sqrt{E_s}\sum_{i=1}^{N}\beta_{\hat{w},i}\exp\left\{\jmath\left(\psi_{w,i} - \psi_{\hat{w},i}\right)\right\} + n_{\hat{w}} \sim \mathcal{CN}\left(N\sqrt{E_s}\mu\,,\, NE_s\sigma_h^2 + N_0\right), \quad (10a)$$

$$\Re\left(\sqrt{E_s}\sum_{i=1}^{N}\beta_{w,i} + n_w\right) \sim \mathcal{N}\left(\frac{N\sigma_h\sqrt{\pi E_s}}{2}L_{1/2}\left(-k\right), NE_s\sigma_h^2\left(1 + k - \frac{\pi}{4}L_{1/2}^2\left(-k\right)\right) + \frac{N_0}{2}\right), \quad (10b)$$

where $L_{1/2}(\cdot)$ denotes the Laguerre polynomial, and

$$\Im\left(\sqrt{E_s}\sum_{i=1}^{N}\beta_{w,i} + n_w\right) \sim \mathcal{N}\left(0, \frac{N_0}{2}\right), \quad (11)$$

where $\Re(\cdot)$ and $\Im(\cdot)$ denote the real part and imaginary part operators, respectively.

We can alternatively express the PPED in (9) as

$$\Pr\left\{|z_w|^2 < |z_{\hat{w}}|^2\right\} = \Pr\left\{X_{ssk} < Y_{ssk}\right\}, \quad (12)$$

where

$$X_{ssk} = \left|\sqrt{E_s}\sum_{i=1}^{N}\beta_{w,i} + n_w\right|^2,$$

$$Y_{ssk} = \left|\sqrt{E_s}\sum_{i=1}^{N}\beta_{\hat{w},i}\exp\left\{\jmath\left(\psi_{w,i} - \psi_{\hat{w},i}\right)\right\} + n_{\hat{w}}\right|^2.$$

From (10) and (11), the variable X_{ssk} can further be modeled as

$$X_{ssk} = \left|(W_0 + W_1) + \jmath W_2\right|^2, \quad (13)$$

where W_0, W_1, and W_2 are independent random variables, whose distributions are given by

$$W_0 \sim \mathcal{N}\left(\mu_X, b\right)\ ,\ W_1, W_2 \sim \mathcal{N}\left(0, c\right), \quad (14)$$

where

$$\mu_X = \frac{N\sigma_h\sqrt{\pi E_s}}{2}L_{\frac{1}{2}}(-k),\ b = NE_s\sigma_h^2\left(1 + k - \frac{\pi}{4}L_{\frac{1}{2}}^2(-k)\right),\ c = \frac{N_0}{2}, \quad (15)$$

using which, the c.f. of X_{ssk} can be expressed as

$$\Psi_{X_{ssk}}\left(\jmath\omega\right) = \frac{\exp\left\{\frac{\jmath\omega\mu_X^2}{1 - 2\jmath\omega(b+c)}\right\}}{\left(1 - 2\jmath\omega\left(b + c\right)\right)^{\frac{1}{2}}\left(1 - 2\jmath\omega c\right)^{\frac{1}{2}}}. \quad (16)$$

The statistics thus obtained for X_{ssk} and Y_{ssk} are utilized to derive the expression of the PPED, as given by the following theorem.

Theorem 1: The expression of the PPED in (12) can be computed as given in (17) shown at the top of the next page, where $\Gamma_{av} \triangleq E_s\sigma_h^2/N_0$ is defined as the average SNR per receive diversity branch and the summation over the set $\sum_{S_{q,\ell+p+1}}$ is carried out for all the possible tuples of $q_1, \ldots, q_{\ell+p+1}$ such that $\sum_{r=1}^{\ell+p+1} rq_r = \ell + p + 1$.

Proof: The proof is given in Appendix I. ■

B. PED Analysis

We now wish to compute the expression of the PED in a similar manner. Let $Y_{ssk_1}, \ldots, Y_{ssk_L}$ denote the expression corresponding to (12) and (9) for all the non-target antennas at the receiver end with $L = N_{R_X} - 1$. It is observed that $Y_{ssk_1}, \ldots, Y_{ssk_L}$ are statistically i.i.d.. Thus, the probability of erroneous detection, denoted by $P_{e,ssk}$, utilizing the greedy detector in (5), is expressed as

$$P_{e,ssk} = 1 - \Pr\left\{Y_{ssk_1}, \ldots, Y_{ssk_L} < X_{ssk}\right\} = 1 - \int_{-\infty}^{\infty}\left(\prod_{i=1}^{L}F_{Y_{ssk_i}}\left(x\right)\right)f_{X_{ssk}}\left(x\right)\mathrm{d}x. \quad (18)$$

$$\Pr\{X_{ssk} < Y_{ssk}\} = 1 - \exp\left\{-\frac{kN^2\Gamma_{av}}{N\Gamma_{av}+1}\right\} \sum_{\ell=0}^{\infty}\sum_{p=0}^{\infty} \frac{(-1)^p \left(kN^2\Gamma_{av}\right)^{\ell} (\ell+p)!}{\left(N\Gamma_{av}+1\right)^{2\ell+p+1} (\ell!)^2\, p!} \sum_{S_{q,\ell+p+1}} \prod_{r=1}^{\ell+p+1} \frac{1}{q_r!}$$
$$\times \left[\frac{2^{r-1}}{r}\left[\frac{r\pi N^2\Gamma_{av}}{4} L_{1/2}^2(-k)\left(N\Gamma_{av}\left(1+k-\frac{\pi}{4}L_{1/2}^2(-k)\right)+\frac{1}{2}\right)^{r-1} + \left(N\Gamma_{av}\left(1+k-\frac{\pi}{4}L_{1/2}^2(-k)\right)+\frac{1}{2}\right)^{r} + \frac{1}{2^r}\right]\right]^{q_r} \quad (17)$$

Furthermore, using similar steps as in (63) (see Appendix I), we have

$$\begin{aligned}
&\prod_{i=1}^{L} F_{Y_{ssk_i}}(x) \\
&= \int_0^x \cdots \int_0^x \frac{\exp\left\{-\frac{y_1+E_sN^2|\mu|^2}{N\sigma_h^2E_s+N_0}\right\}}{N\sigma_hE_s+N_0} I_0\left(\frac{2\sqrt{E_sN^2|\mu|^2y_1}}{N\sigma_h^2E_s+N_0}\right) \\
&\quad \ldots \times \frac{\exp\left\{-\frac{y_L+E_sN^2|\mu|^2}{N\sigma_h^2E_s+N_0}\right\}}{N\sigma_hE_s+N_0} I_0\left(\frac{2\sqrt{E_sN^2|\mu|^2y_L}}{N\sigma_h^2E_s+N_0}\right) \mathrm{d}y_1 \ldots \mathrm{d}y_L \\
&\overset{(a)}{=} \exp\left\{-\frac{LE_sN^2|\mu|^2}{NE_s\sigma_h^2+N_0}\right\} \sum_{\ell_1=0}^{\infty}\cdots\sum_{\ell_L=0}^{\infty}\sum_{p_1=0}^{\infty}\cdots\sum_{p_L=0}^{\infty} \\
&\quad \times \frac{(-1)^{\sum_{i=1}^{L} p_i} \left(E_sN^2|\mu|^2\right)^{\sum_{i=1}^{L}\ell_i} \prod_{i=1}^{L}\int_0^x \left[y_i^{\ell_i+p_i}\mathrm{d}y_i\right]}{\left(NE_s\sigma_h^2+N_0\right)^{L+\sum_{i=1}^{L}2\ell_i+p_i} \prod_{i=1}^{L}(\ell_i!)^2\, p_i!} \\
&\overset{(b)}{=} \exp\left\{-\frac{LE_sN^2|\mu|^2}{NE_s\sigma_h^2+N_0}\right\} \sum_{\ell_1=0}^{\infty}\cdots\sum_{\ell_L=0}^{\infty}\sum_{p_1=0}^{\infty}\cdots\sum_{p_L=0}^{\infty} \\
&\quad \times \frac{(-1)^{\sum_{i=1}^{L} p_i} \left(E_sN^2|\mu|^2\right)^{\sum_{i=1}^{L}\ell_i} x^{\sum_{i=1}^{L}(\ell_i+p_i+1)}}{\left(NE_s\sigma_h^2+N_0\right)^{L+\sum_{i=1}^{L}2\ell_i+p_i} \prod_{i=1}^{L}(\ell_i!)^2\, p_i!\,(\ell_i+p_i+1)},
\end{aligned} \quad (19)$$

where (a) is obtained by using the series-form expansions of $I_0(x)$ and $\exp\{x\}$ in (64).

Upon substituting (19) in (18) to obtain the expression of $P_{e,ssk}$, we finally need to solve the integration given as

$$\begin{aligned}
\int_0^{\infty} x^{\sum_{i=1}^{L}(\ell_i+p_i+1)} f_{X_{ssk}}(x)\mathrm{d}x &= \mathbf{E}\left[X_{ssk}^{\sum_{i=1}^{L}(\ell_i+p_i+1)}\right] \\
&= \frac{1}{\jmath^{\sum_{i=1}^{L}(\ell_i+p_i+1)}} \left[\frac{\partial^{\sum_{i=1}^{L}(\ell_i+p_i+1)}}{\partial\omega^{\sum_{i=1}^{L}(\ell_i+p_i+1)}} \Psi_{X_{ssk}}(\jmath\omega)\right]\Bigg|_{\omega=0}.
\end{aligned} \quad (20)$$

The expression in (20) is similar to that obtained in (66). Thus, following similar steps from (68)-(69) and by using Faa-di Bruno's formula, the series-form expression for the probability of erroneous antenna detection $P_{e,ssk}$ is given in (21), as shown at the top of the next page, where $\alpha_{\ell,p} = \sum_{i=1}^{L}(\ell_i+p_i+1)$ and the summation over the set $S_{q,\alpha_{\ell,p}}$ is carried out for all possible tuples of $q_1 \ldots, q_{\alpha_{\ell,p}}$ such that $\sum_{r=1}^{\ell+p+1} rq_r = \alpha_{\ell,p}$.

C. Asymptotic Analysis

Assuming a high average SNR per branch, i.e., $\Gamma_{av} \gg 1$, the expression of $P_{e,ssk}$ in (21) simplifies to

$$\begin{aligned}
P_{e,ssk_{\Gamma_{av}\gg 1}} &= 1 - e^{-kLN} \sum_{\ell_1=0}^{\infty}\cdots\sum_{\ell_L=0}^{\infty}\sum_{p_1=0}^{\infty}\cdots\sum_{p_L=0}^{\infty} (-1)^{\sum_{i=1}^{L}p_i} (kN)^{\sum_{i=1}^{L}\ell_i} \\
&\quad \times \frac{\prod_{i=1}^{L}(\ell_i+p_i)!}{\prod_{i=1}^{L}(\ell_i!)^2\, p_i!} \sum_{\substack{q_1\ldots,q_{\alpha_{\ell,p}} \\ 0\le q_1,\ldots,q_{\alpha_{\ell,p}}\le\alpha_{\ell,p} \\ q_1+2q_2+\ldots+\alpha_{\ell,p}q_{\alpha_{\ell,p}}=\alpha_{\ell,p}}} \prod_{r=1}^{\alpha_{\ell,p}} \frac{1}{q_r!}\left[\frac{2^{r-1}}{r}\right. \\
&\quad \times \left[\frac{r\pi N}{4}L_{1/2}^2(-k)\left(1+k-\frac{\pi}{4}L_{1/2}^2(-k)\right)^{r-1} \right. \\
&\quad \left.\left. + \left(1+k-\frac{\pi}{4}L_{1/2}^2(-k)\right)^{r}\right]\right]^{q_r}.
\end{aligned} \quad (22)$$

Remark 1: It can be observed from (22) that $P_{e,ssk}\big|_{\Gamma_{av}\gg 1}$ is independent of Γ_{av} implying that the PED of the considered RIS-assisted SSK system saturates to the value obtained in (22) at high Γ_{av}.

Similarly, assuming that the average SNR per branch is very small, i.e., $\Gamma_{av} \ll 1$, the PED in (21) simplifies to

$$\begin{aligned}
P_{e,ssk_{\Gamma_{av}\ll 1}} &= 1 - e^{-kLN^2\Gamma_{av}} \\
&\quad \times \sum_{\ell_1=0}^{\infty}\cdots\sum_{\ell_L=0}^{\infty}\sum_{p_1=0}^{\infty}\cdots\sum_{p_L=0}^{\infty} (-1)^{\sum_{i=1}^{L}p_i} \left(kN^2\Gamma_{av}\right)^{\sum_{i=1}^{L}\ell_i} \\
&\quad \times \frac{\prod_{i=1}^{L}(\ell_i+p_i)!}{\prod_{i=1}^{L}(\ell_i!)^2\, p_i!} \sum_{\substack{q_1\ldots,q_{\alpha_{\ell,p}} \\ 0\le q_1,\ldots,q_{\alpha_{\ell,p}}\le\alpha_{\ell,p} \\ q_1+2q_2+\ldots+\alpha_{\ell,p}q_{\alpha_{\ell,p}}=\alpha_{\ell,p}}} \prod_{r=1}^{\alpha_{\ell,p}} \frac{1}{q_r!r^{q_r}}.
\end{aligned} \quad (23)$$

Finally, if $\Gamma_{av} = 0$, the PED simplifies to

$$\begin{aligned}
P_{e,ssk}\big|_{\Gamma_{av}=0} &= 1 - \sum_{p_1=0}^{\infty}\cdots\sum_{p_L=0}^{\infty} (-1)^{\sum_{i=1}^{L}p_i} \\
&\quad \times \sum_{\substack{q_1\ldots,q_{\sum_{i=1}^{L}(p_i+1)} \\ 0\le q_1,\ldots,q_{\sum_{i=1}^{L}(p_i+1)}\le\sum_{i=1}^{L}(p_i+1) \\ q_1+2q_2+\ldots+\left(\sum_{i=1}^{L}(p_i+1)\right)q_{\sum_{i=1}^{L}(p_i+1)}=\sum_{i=1}^{L}(p_i+1)}} \prod_{r=1}^{\sum_{i=1}^{L}(p_i+1)} \frac{1}{q_r!r^{q_r}},
\end{aligned} \quad (24)$$

where the summation over the set $\sum_{S_{q,\sum_{i=1}^{L}(p_i+1)}}$ is carried

$$P_{e,ssk} = 1-\exp\left\{-\frac{kLN^2\Gamma_{av}}{N\Gamma_{av}+1}\right\}\sum_{\ell_1,\ldots,\ell_L=0}^{\infty}\sum_{p_1,\ldots,p_L=0}^{\infty}\frac{(-1)^{\sum_{i=1}^{L}p_i}\left(kN^2\Gamma_{av}\right)^{\sum_{i=1}^{L}\ell_i}\prod_{i=1}^{L}(\ell_i+p_i)!}{(N\Gamma_{av}+1)^{\alpha_{\ell,p}+\sum_{i=1}^{L}\ell_i}\prod_{i=1}^{L}(\ell_i!)^2 p_i!}$$
$$\times\sum_{S_{q,\alpha_{\ell,p}}}\prod_{r=1}^{\alpha_{\ell,p}}\frac{1}{q_r!}\left[\frac{2^{r-1}}{r}\left[\frac{r\pi N^2\Gamma_{av}}{4}L_{1/2}^2(-k)\left(N\Gamma_{av}\left(1+k-\frac{\pi}{4}L_{1/2}^2(-k)\right)+\frac{1}{2}\right)^{r-1}\right.\right.$$
$$\left.\left.+\left(N\Gamma_{av}\left(1+k-\frac{\pi}{4}L_{1/2}^2(-k)\right)+\frac{1}{2}\right)^{r}+\frac{1}{2^r}\right]\right]^{q_r} \quad (21)$$

out for all possible tuples of $q_1\ldots,q_{\sum_{i=1}^{L}(p_i+1)}$ such that $\sum_{r=1}^{\sum_{i=1}^{L}(p_i+1)} rq_r=\sum_{i=1}^{L}(p_i+1)$.

IV. PED Analysis of the RIS-Assisted SM System

The performance evaluation of the RIS-SM system follows a similar approach as for the RIS-SSK system and is presented in this section.

A. PPED Analysis

First, we denote by w and $\hat{w}$ the indices corresponding to the target and some other non-target receive diversity branches, and compute the PPED given by

$$\Pr\left\{|z_{w_{sm}}|^2<|z_{\hat{w}_{sm}}|^2\right\}=\Pr\left\{\left|\left(\sum_{i=1}^{N}h_{w,i}e^{\jmath\phi_i}\right)v_\zeta+n_w\right|^2 < \left|\left(\sum_{i=1}^{N}h_{\hat{w},i}e^{\jmath\phi_i}\right)v_\zeta+n_{\hat{w}}\right|^2\right\}, \quad (25)$$

where v_ζ is the data symbol belonging to the M-ary QAM/M-PSK constellation, $\mathbf{E}\left[|v_\zeta|^2\right]=E_s$. Thus, the normalized data symbol, denoted by v with $\mathbf{E}\left[|v|^2\right]=1$, can be expressed as

$$v=v_\zeta/\sqrt{E_s}=\Re(v)+\jmath\Im(v)\ . \quad (26)$$

Similar to the RIS-assisted SSK system, (25) can be expressed in terms of an optimization problem to maximize the signal energy at the target antenna as

$$\min_{\{\phi_i\}_{i=1}^{N}}\ \Pr\left\{\left|\sum_{i=1}^{N}\beta_{\hat{w},i}\exp\left\{\jmath\left(\phi_i-\psi_{\hat{w}_i,i}\right)\right\}v_\zeta\right|^2 > \left|\sum_{i=1}^{N}\beta_{w,i}\exp\left\{\jmath\left(\phi_i-\psi_{w_i,i}\right)\right\}v_\zeta\right|^2\right\}. \quad (27)$$

Furthermore, the result in (27) can be minimized by letting $\phi_i=\psi_{w,i}$ for $i=1,\ldots,N$, resulting in the optimization problem leading to the expression of the PPED in (25) being written as

$$\Pr\left\{|z_{w_{sm}}|^2<|z_{\hat{w}_{sm}}|^2\right\}=\Pr\left\{\left|\sum_{i=1}^{N}\beta_{\hat{w},i}\exp\left\{\jmath\left(\psi_{w,i}-\psi_{\hat{w},i}\right)\right\}v_\zeta+n_{\hat{w}}\right|^2 > \left|\sum_{i=1}^{N}\beta_{w,i}v_\zeta+n_w\right|^2\right\}. \quad (28)$$

To obtain the solution to (28), we first find the statistics of the terms in (28), which can be obtained by using the central limit theorem, as given by [42]

$$\sqrt{E_s}\sum_{i=1}^{N}\beta_{\hat{m},i}\exp\left\{\jmath\left(\psi_{m,i}-\psi_{\hat{m},i}\right)\right\}v+n_{\hat{m}} \sim\mathcal{CN}\left(N\sqrt{E_s}\mu,\ NE_s\sigma_h^2+N_0\right). \quad (29)$$

$$\Re\left(\sqrt{E_s}\sum_{i=1}^{N}\beta_{m,i}v+n_m\right)\sim\mathcal{N}\left(\frac{N\sigma_h\sqrt{\pi E_s}\,(\Re(v))}{2}L_{\frac{1}{2}}(-k),\ NE_s\sigma_h^2(\Re(v))^2\left(1+k-\frac{\pi}{4}L_{\frac{1}{2}}^2(-k)\right)+\frac{N_0}{2}\right), \quad (30)$$

and

$$\Im\left(\sqrt{E_s}\sum_{i=1}^{N}\beta_{m,i}v+n_m\right)\sim\mathcal{N}\left(\frac{N\sigma_h\sqrt{\pi E_s}\,(\Im(v))}{2}L_{\frac{1}{2}}(-k),\ NE_s\sigma_h^2(\Im(v))^2\left(1+k-\frac{\pi}{4}L_{\frac{1}{2}}^2(-k)\right)+\frac{N_0}{2}\right). \quad (31)$$

Further, using the same approach as for the analysis of the RIS-SSK system ((8a) and (8b)), we define two random variables X_{sm} corresponding to the instantaneous signal energy at the target antenna (related to $|z_{w_{sm}}|^2$) and Y_{sm} corresponding to the instantaneous signal energy at any other non-target antenna (related to $|z_{\hat{w}_{sm}}|^2$), where X_{sm} can be statistically modeled as

$$X_{sm}=|(V_a+V_1)+\jmath(V_b+V_2)|^2, \quad (32)$$

with V_a, V_b, V_1, and V_2 being independent random variables, whose distribution can be obtained from (29)-(31) as

$$V_1,V_2\sim\mathcal{N}(0,c)\ ,\ V_a\sim\mathcal{N}(\mu_1,b_1)\ ,\ V_b\sim\mathcal{N}(\mu_2,b_2)\ , \quad (33a)$$

where

$$\mu_1 = \mu_x \Re(v), \mu_2 = \mu_x \Im(v), b_1 = b\Re(v)^2, b_2 = b\Im(v)^2, \quad (33b)$$

and the variables μ_X and b are given in (15). Unlike the RIS-assisted SSK scheme, it is observed that the statistics of the terms in (28) are dependent on the constellation of the transmitted symbol v. Moreover, similar to the RIS-assisted SSK scheme, the c.f. of X_{sm} can be written as

$$\psi_{X_{sm}}(\jmath\omega) = \frac{\exp\left\{\frac{\jmath\omega\mu_1^2}{1-2\jmath\omega(b_1+c)} + \frac{\jmath\omega\mu_2^2}{1-2\jmath\omega(b_2+c)}\right\}}{(1-2\jmath\omega(b_1+c))^{\frac{1}{2}}(1-2\jmath\omega(b_2+c))^{\frac{1}{2}}}. \quad (34)$$

The statistics thus obtained for X_{sm} and Y_{sm} are utilized to derive the expression of the PPED, as given by the following theorem.

Theorem 2: The expression of the PPED for the RIS-assisted SM is given in (35), shown at the top of the next page.

Proof: The proof is given in Appendix II. ■

B. PED Analysis

We now wish to compute the PED. Let $Y_{sm_1}, \ldots, Y_{sm_L}$ denote the expression corresponding to (28) for all the L non-target antennas at the receiver end with $L = N_{R_X} - 1$. It can be observed that $Y_{sm_1}, \ldots, Y_{sm_L}$ are statistically i.i.d.. Thus, the probability of erroneous detection, denoted by $P_{e,sm}$, utilizing the greedy detector in (5), is expressed as

$$\begin{aligned} P_{e,sm} &= 1 - \Pr\{Y_{sm_1}, \ldots, Y_{sm_L} < X_{sm}\} \\ &= 1 - \int_{-\infty}^{\infty} \left(\prod_{i=1}^{L} F_{Y_{sm_i}}(x)\right) f_{X_{sm}}(x)\,\mathrm{d}x. \end{aligned} \quad (36)$$

Similar to the RIS-assisted SSK system, the product term in (36) can be computed as

$$\begin{aligned} &\prod_{i=1}^{L} F_{Y_{sm_i}}(x) \\ &= \int_0^x \cdots \int_0^x \frac{\exp\left\{-\frac{y_1 + E_s N^2 |\mu|^2}{N\sigma_h^2 E_s + N_0}\right\}}{N\sigma_h E_s + N_0} I_0\left(\frac{2\sqrt{E_s N^2 |\mu|^2 y_1}}{N\sigma_h^2 E_s + N_0}\right) \\ &\quad \ldots \times \frac{\exp\left\{-\frac{y_L + E_s N^2 |\mu|^2}{N\sigma_h^2 E_s + N_0}\right\}}{N\sigma_h E_s + N_0} I_0\left(\frac{2\sqrt{E_s N^2 |\mu|^2 y_L}}{N\sigma_h^2 E_s + N_0}\right) \mathrm{d}y_1 \ldots \mathrm{d}y_L \\ &\overset{(a)}{=} \exp\left\{-\frac{L E_s N^2 |\mu|^2}{N E_s \sigma_h^2 + N_0}\right\} \sum_{\ell_1=0}^{\infty} \cdots \sum_{\ell_L=0}^{\infty} \sum_{p_1=0}^{\infty} \cdots \sum_{p_L=0}^{\infty} \\ &\quad \times \frac{(-1)^{\sum_{i=1}^{L} p_i} \left(E_s N^2 |\mu|^2\right)^{\sum_{i=1}^{L} \ell_i} \prod_{i=1}^{L} \int_0^x \left[y_i^{\ell_i + p_i} \mathrm{d}y_i\right]}{(N E_s \sigma_h^2 + N_0)^{L + \sum_{i=1}^{L} 2\ell_i + p_i} \prod_{i=1}^{L} (\ell_i!)^2 p_i!} \\ &\overset{(b)}{=} \exp\left\{-\frac{L E_s N^2 |\mu|^2}{N E_s \sigma_h^2 + N_0}\right\} \sum_{\ell_1=0}^{\infty} \cdots \sum_{\ell_L=0}^{\infty} \sum_{p_1=0}^{\infty} \cdots \sum_{p_L=0}^{\infty} \\ &\quad \times \frac{(-1)^{\sum_{i=1}^{L} p_i} \left(E_s N^2 |\mu|^2\right)^{\sum_{i=1}^{L} \ell_i} x^{\sum_{i=1}^{L} (\ell_i + p_i + 1)}}{(N E_s \sigma_h^2 + N_0)^{L + \sum_{i=1}^{L} 2\ell_i + p_i} \prod_{i=1}^{L} (\ell_i!)^2 p_i! (\ell_i + p_i + 1)}, \end{aligned} \quad (37)$$

where the step (a) is obtained by using the series-form expansions of $I_0(x)$ and $\exp\{x\}$ in (64). Substituting (37) in (36) and using some algebraic simplifications results in the series-form expression of $P_{e,sm}$ given in (38) shown at the top of the next page.

C. Asymptotic Analysis

Assuming a low average SNR, i.e. $\Gamma_{av} \ll 1$, the $P_{e,sm}$ in (38) simplifies to

$$\begin{aligned} &P_{e_{sm}, \Gamma_{av} \ll 1} \\ &= 1 - \left\{e^{-kLN}\right\} \sum_{\ell_1=0}^{\infty} \cdots \sum_{\ell_L=0}^{\infty} \sum_{p_1=0}^{\infty} \cdots \sum_{p_L=0}^{\infty} (-1)^{\sum_{i=1}^{L} p_i} \\ &\quad \times \frac{\left(kN^2\Gamma_{av}\right)^{\sum_{i=1}^{L} \ell_i} \prod_{i=1}^{L} (\ell_i + p_i)!}{\prod_{i=1}^{L} (\ell_i!)^2 p_i!} \\ &\quad \sum_{q_1, \ldots, q_{\alpha_{\ell,p}}}^{\alpha_{\ell,p}} \prod_{r=1}^{} \frac{1}{q_r!} \left[\frac{1}{r}\left[\left(\frac{r\pi N^2 \Gamma_{av} (\Re(v))^2}{4} L_{\frac{1}{2}}^2(-k)\right)\right.\right. \\ &\quad \left.\left. + \left(\frac{r\pi N^2 (\Im(v))^2}{4} L_{1/2}^2(-k)\right) + 1\right]\right]^{q_r}. \end{aligned} \quad (39)$$

$$0 \le q_1, \ldots, q_{\alpha_{\ell,p}} \le \alpha_{\ell,p}, \quad q_1 + 2q_2 + \ldots + (\alpha_{\ell,p}) q_{\alpha_{\ell,p}} = \alpha_{\ell,p}$$

Also, assuming a high average SNR, i.e. $\Gamma_{av} \gg 1$, $P_{e,sm}$ in (38) simplifies as given in (40) shown in the next page.

Remark 2: Similar to the RIS-assisted SSK system, it can be observed from (39) that the expression of $P_{e,sm}\big|_{\Gamma_{av} \gg 1}$ *is independent of* Γ_{av}*, thus implying that the PED of the considered RIS-assisted SM system saturates to the value obtained in (39) at high* Γ_{av}*.*

Additionally, if $\Gamma_{av} = 0$, the expression of the PED in (38) is obtained as

$$\begin{aligned} P_{e,sm_{\Gamma_{av}=0}} &= 1 - \sum_{p_1=0}^{\infty} \cdots \sum_{p_L=0}^{\infty} (-1)^{\sum_{i=1}^{L} p_i} \\ &\quad \times \sum_{q_1, \ldots, q_{\sum_{i=1}^{L}(p_i+1)}} \prod_{r=1}^{\sum_{i=1}^{L}(p_i+1)} \frac{1}{q_r! r^{q_r}}. \end{aligned} \quad (41)$$

$$0 \le q_1, \ldots, q_{\sum_{i=1}^{L}(p_i+1)} \le \sum_{i=1}^{L}(p_i+1), \quad q_1 + 2q_2 + \ldots + \left(\sum_{i=1}^{L}(p_i+1)\right) q_{\sum_{i=1}^{L}(p_i+1)} = \sum_{i=1}^{L}(p_i+1)$$

Remark 3: It can be noted by comparing (41) and (24) that the performance of the RIS-assisted SSK and the SM systems are the same if $\Gamma_{av} = 0$*. Intuitively, this is an expected result as the SSK scheme differs from the SM scheme in terms of the constellation utilized for data transmission, and for* $\Gamma_{av} = 0$*, the transmitted energy is zero.*

V. SEP Analysis of the RIS-Assisted System

In this section, we compute the SEP of the RIS-assisted system when the transmitter employs the M-ary QAM and

$$\Pr\{X_{sm}<Y_{sm}\} = 1-\exp\left\{-\frac{kN^2\Gamma_{av}}{N\Gamma_{av}+1}\right\}\sum_{\ell=0}^{\infty}\sum_{p=0}^{\infty}\frac{(-1)^p\left(kN^2\Gamma_{av}\right)^{\ell}(\ell+p)!}{\left(N\Gamma_{av}+1\right)^{2\ell+p+1}\left(\ell!\right)^2 p!}$$
$$\sum_{\substack{q_1\ldots,q_{\ell+p+1}\\ 0\le q_1,\ldots,q_{\ell+p+1}\le \ell+p+1\\ q_1+2q_2+\ldots+(\ell+p+1)q_{\ell+p+1}=\ell+p+1}}\prod_{r=1}^{\ell+p+1}\frac{1}{q_r!}\left[\frac{2^{r-1}}{r}\left[\frac{r\pi N^2\Gamma_{av}\left(\Re(v)\right)^2}{4}L_{1/2}^2(-k)\left(N\Gamma_{av}\left(\Re(v)\right)^2\left(1+k-\frac{\pi}{4}L_{1/2}^2(-k)\right)+\frac{1}{2}\right)^{r-1}\right.\right.$$
$$+\frac{r\pi N^2\Gamma_{av}\left(\Im(v)\right)^2}{4}L_{1/2}^2(-k)\left(N\Gamma_{av}\left(\Im(v)\right)^2\left(1+k-\frac{\pi}{4}L_{1/2}^2(-k)\right)+\frac{1}{2}\right)^{r-1}$$
$$\left.\left.+\left(N\Gamma_{av}\left(\Re(v)\right)^2\left(1+k-\frac{\pi}{4}L_{1/2}^2(-k)\right)+\frac{1}{2}\right)^{r}+\left(N\Gamma_{av}\left(\Im(v)\right)^2\left(1+k-\frac{\pi}{4}L_{1/2}^2(-k)\right)+\frac{1}{2}\right)^{r}\right]\right]^{q_r} \quad (35)$$

$$P_{e_{sm}} = 1-\exp\left\{-\frac{kLN^2\Gamma_{av}}{N\Gamma_{av}+1}\right\}\sum_{\ell_1=0}^{\infty}\cdots\sum_{\ell_L=0}^{\infty}\sum_{p_1=0}^{\infty}\cdots\sum_{p_L=0}^{\infty}\frac{(-1)^{\sum_{i=1}^{L}p_i}\left(kN^2\Gamma_{av}\right)^{\sum_{i=1}^{L}\ell_i}\prod_{i=1}^{L}(\ell_i+p_i)!}{\left(N\Gamma_{av}+1\right)^{L+\sum_{i=1}^{L}2\ell_i+p_i}\prod_{i=1}^{L}\left(\ell_i!\right)^2 p_i!}$$
$$\times\sum_{\substack{q_1\ldots,q_{\alpha_{\ell,p}}\\ 0\le q_1,\ldots,q_{\alpha_{\ell,p}}\le\alpha_{\ell,p}\\ q_1+2q_2+\ldots+(\alpha_{\ell,p})q_{\alpha_{\ell,p}}=\alpha_{\ell,p}}}\prod_{r=1}^{\sum_{i=1}^{L}\alpha_{\ell,p}}\frac{1}{q_r!}\left[\frac{2^{r-1}}{r}\left[\frac{r\pi N^2\Gamma_{av}\left(\Re(v)\right)^2}{4}L_{1/2}^2(-k)\left(N\Gamma_{av}\left(\Re(v)\right)^2\left(1+k-\frac{\pi}{4}L_{1/2}^2(-k)\right)+\frac{1}{2}\right)^{r-1}\right.\right.$$
$$+\frac{r\pi N^2\Gamma_{av}\left(\Im(v)\right)^2}{4}L_{1/2}^2(-k)\left(N\Gamma_{av}\left(\Im(v)\right)^2\left(1+k-\frac{\pi}{4}L_{1/2}^2(-k)\right)+\frac{1}{2}\right)^{r-1}$$
$$\left.\left.+\left(N\Gamma_{av}\left(\Re(v)\right)^2\left(1+k-\frac{\pi}{4}L_{1/2}^2(-k)\right)+\frac{1}{2}\right)^{r}+\left(N\Gamma_{av}\left(\Im(v)\right)^2\left(1+k-\frac{\pi}{4}L_{1/2}^2(-k)\right)+\frac{1}{2}\right)^{r}\right]\right]^{q_r} \quad (38)$$

$$P_{e_{sm},\Gamma_{av}\gg 1} = 1-\exp\{-kLN\}\sum_{\ell_1=0}^{\infty}\cdots\sum_{\ell_L=0}^{\infty}\sum_{p_1=0}^{\infty}\cdots\sum_{p_L=0}^{\infty}\frac{(-1)^{\sum_{i=1}^{L}p_i}\left(kN^2\right)^{\sum_{i=1}^{L}\ell_i}\prod_{i=1}^{L}(\ell_i+p_i)!}{(N)^{L+\sum_{i=1}^{L}2\ell_i+p_i}\prod_{i=1}^{L}\left(\ell_i!\right)^2 p_i!}$$
$$\times\sum_{\substack{q_1\ldots,q_{\alpha_{\ell,p}}\\ 0\le q_1,\ldots,q_{\alpha_{\ell,p}}\le\alpha_{\ell,p}\\ q_1+2q_2+\ldots+(\alpha_{\ell,p})q_{\alpha_{\ell,p}}=\alpha_{\ell,p}}}\prod_{r=1}^{\sum_{i=1}^{L}\alpha_{\ell,p}}\frac{1}{q_r!}\left[\frac{2^{r-1}}{r}\left[\frac{r\pi N^2\left(\Re(v)\right)^2}{4}L_{1/2}^2(-k)\left(N\left(\Re(v)\right)^2\left(1+k-\frac{\pi}{4}L_{1/2}^2(-k)\right)\right)^{r-1}\right.\right.$$
$$+\frac{r\pi N^2\left(\Im(v)\right)^2}{4}L_{1/2}^2(-k)\left(N\left(\Im(v)\right)^2\left(1+k-\frac{\pi}{4}L_{1/2}^2(-k)\right)\right)^{r-1}$$
$$\left.\left.+\left(N\left(\Re(v)\right)^2\left(1+k-\frac{\pi}{4}L_{1/2}^2(-k)\right)\right)^{r}+\left(N\left(\Im(v)\right)^2\left(1+k-\frac{\pi}{4}L_{1/2}^2(-k)\right)\right)^{r}\right]\right]^{q_r} \quad (40)$$

M-PSK constellations for data transmission. The RIS elements introduce phase shifts on the transmitted signal such that the instantaneous SNR at the receiver is maximized, as given in (3). In the case of a large number of RIS elements, i.e., $N \gg 1$, the square root of the maximum instantaneous SNR, denoted by γ, follows a Gaussian distribution as

$$\sqrt{\gamma} \sim \mathcal{N}\left(\frac{NL_{1/2}(-k)\sqrt{\Gamma_{av}\pi}}{2}, N\Gamma_{av}(1+k-\frac{\pi}{4}L_{1/2}^2(-k))\right). \quad (42)$$

It is to be noted that the distribution of γ is the same as $\gamma_{w,max}, \forall w \in \{1,\ldots,N_{R_X}\}$. Furthermore, from (42), it is observed that γ follows a non-central $\chi^2(1)$ distribution and thus, its c.f. is given by

$$\Psi_\gamma(\jmath\omega) = \frac{\exp\left\{\frac{\frac{\jmath\omega N^2\pi\Gamma_{av}L_{1/2}^2(-k)}{4}}{1-2\jmath\omega N\Gamma_{av}(1+k-\frac{\pi}{4}L_{1/2}^2(-k))}\right\}}{\left(1-2\jmath\omega N\Gamma_{av}\left(1+k-\frac{\pi}{4}L_{1/2}^2(-k)\right)\right)^{\frac{1}{2}}}. \quad (43)$$

A. SEP for M-PSK Constellation

Using the c.f. of γ in (43), the SEP of the RIS-assisted system employing an M-PSK constellation can be expressed as [18]

$$P_{s,M\text{-PSK}} = \frac{1}{\pi}\int_0^{\frac{M-1}{M}\pi}\Psi_\gamma\left(\frac{-\sin^2\frac{\pi}{M}}{\sin^2\eta}\right)\mathrm{d}\eta. \quad (44)$$

Substituting (43) in (44), the SEP can be obtained by computing

$$P_{s,M\text{-PSK}} = \frac{1}{\pi}\int_0^{\frac{M-1}{M}\pi}\frac{\exp\left\{-\frac{\frac{\sin^2\frac{\pi}{M}}{\sin^2\eta}N^2\pi\Gamma_{av}L_{1/2}^2(-k)}{1+2\frac{\sin^2\frac{\pi}{M}}{\sin^2\eta}N\Gamma_{av}(1+k-\frac{\pi}{4}L_{1/2}(-k))}\right\}}{\left(1+2\frac{\sin^2\frac{\pi}{M}}{\sin^2\eta}N\Gamma_{av}(1+k-\frac{\pi}{4}L_{1/2}^2(-k))\right)^{\frac{1}{2}}}\mathrm{d}\eta. \quad (45)$$

By assuming a high average SNR, i.e., $\Gamma_{av} \gg 1$, we have

$$1+2\frac{\sin^2\frac{\pi}{M}}{\sin^2\eta}N\Gamma_{av}\left(1+k-\frac{\pi}{4}L_{1/2}^2(-k)\right) \approx 2\frac{\sin^2\frac{\pi}{M}}{\sin^2\eta}N\Gamma_{av}\left(1+k-\frac{\pi}{4}L_{1/2}^2(-k)\right). \quad (46)$$

Therefore, the asymptotic expression of the SEP at high Γ_{av} is obtained as

$$P_{s,M\text{-PSK}}\big|_{\Gamma_{av}\gg 1} \approx \frac{1-\cos\left(\frac{M-1}{M}\right)\pi}{\pi\left(2N\Gamma_{av}\left(1+k-\frac{\pi}{4}L_{1/2}^2(-k)\right)\right)^{\frac{1}{2}}} \times \exp\left\{\frac{-N\pi L_{1/2}^2(-k)}{8\left(1+k-\frac{\pi}{4}L_{1/2}^2(-k)\right)}\right\}. \quad (47)$$

Assuming a low SNR $\Gamma_{av} \ll 1$ and $M = 2$ we have

$$1+2\frac{\sin^2\frac{\pi}{M}}{\sin^2\eta}N\Gamma_{av}\left(1+k-\frac{\pi}{4}L_{1/2}^2(-k)\right) \approx 1, \quad (48)$$

which, when substituted in (45), results in the following SEP:

$$P_{s,M\text{-PSK}}\big|_{\Gamma_{av}\ll 1, M=2} \approx Q\left(\sqrt{\frac{N^2\pi\Gamma_{av}L_{1/2}^2(-k)}{2}}\right), \quad (49)$$

where $Q(\cdot)$ denotes the Gaussian-Q function. Additionally, if $M > 2$, the corresponding approximation becomes

$$\frac{\exp\left\{-\frac{\frac{\sin^2\frac{\pi}{M}}{\sin^2\eta}N^2\pi\Gamma_{av}L_{1/2}^2(-k)}{1+2\frac{\sin^2\frac{\pi}{M}}{\sin^2\eta}N\Gamma_{av}(1+k-\frac{\pi}{4}L_{1/2}(-k))}\right\}}{\left(1+2\frac{\sin^2\frac{\pi}{M}}{\sin^2\eta}N\Gamma_{av}(1+k-\frac{\pi}{4}L_{1/2}^2(-k))\right)^{\frac{1}{2}}} \approx \exp\left\{-\frac{\frac{\sin^2\frac{\pi}{M}}{\sin^2\eta}N^2\pi\Gamma_{av}L_{1/2}^2(-k)}{1+2\frac{\sin^2\frac{\pi}{M}}{\sin^2\eta}N\Gamma_{av}(1+k-\frac{\pi}{4}L_{1/2}(-k))}\right\}, \quad (50)$$

which, when substituted in (45), results in the asymptotic expression of the SEP as follows:

$$P_{s,M\text{-PSK}}\big|_{\Gamma_{av}\ll 1, M>2} \approx \frac{(M-1)}{M} - \frac{NL_{1/2}^2(-k)}{8\left(1+k-\frac{\pi}{4}L_{1/2}^2(-k)\right)\sqrt{1+\zeta_M}} \times\left[\tan^{-1}\left(\sqrt{1+\zeta_M}\tan\left(\frac{(M-1)\pi}{M}\right)\right) + \frac{\sqrt{1+\zeta_M}}{2}\tan\left(\frac{(M-1)\pi}{M}\right)\right], \quad (51)$$

where

$$\zeta_M = \frac{1}{2\sin^2\frac{\pi}{M}N\Gamma_{av}\left(1+k-\frac{\pi}{4}L_{1/2}^2(-k)\right)}. \quad (52)$$

B. SEP for M-QAM Constellation

Using the c.f. of γ in (43), the SEP of the RIS-assisted system employing M-ary QAM for data modulation can be expressed as

$$P_{s,M\text{-QAM}} = \frac{4}{\pi}\left(1-\frac{1}{\sqrt{M}}\right)\int_0^{\frac{\pi}{2}}\Psi_\gamma\left(\frac{-3}{2(M-1)\sin^2\eta}\right)\mathrm{d}\eta - \frac{4}{\pi}\left(1-\frac{1}{\sqrt{M}}\right)^2\int_0^{\frac{\pi}{4}}\Psi_\gamma\left(\frac{-3}{2(M-1)\sin^2\eta}\right)\mathrm{d}\eta, \quad (53)$$

which using (43) can be re-written as given in (54), shown at the top of the next page.

Assuming high average SNR values, i.e., $\Gamma_{av} \gg 1$, (54) can be simplified using the approximation

$$1+\frac{3N\Gamma_{av}}{(M-1)\sin^2\eta}\left(1+k-\frac{\pi}{4}L_{1/2}^2(-k)\right) \approx \frac{3N\Gamma_{av}}{(M-1)\sin^2\eta}\left(1+k-\frac{\pi}{4}L_{1/2}^2(-k)\right). \quad (55)$$

Therefore, the asymptotic expression of the SEP can be

$$P_{s,M\text{-QAM}}=\frac{4}{\pi}\left(1-\frac{1}{\sqrt{M}}\right)\int_0^{\frac{\pi}{2}}\frac{\exp\left\{\frac{-\frac{3N^2\Gamma_{av}\pi}{8(M-1)\sin^2\eta}L_{1/2}^2(-k)}{1+\frac{3N\Gamma_{av}}{(M-1)\sin^2\eta}\left(1+k-\frac{\pi}{4}L_{1/2}^2(-k)\right)}\right\}\mathrm{d}\eta}{\left(1+\frac{3N\Gamma_{av}}{(M-1)\sin^2\eta}\left(1+k-\frac{\pi}{4}L_{1/2}^2(-k)\right)\right)^{\frac{1}{2}}}-\frac{4}{\pi}\left(1-\frac{1}{\sqrt{M}}\right)^2\int_0^{\frac{\pi}{4}}\frac{\exp\left\{\frac{-\frac{3N^2\Gamma_{av}\pi}{8(M-1)\sin^2\eta}L_{1/2}^2(-k)}{1+\frac{3N\Gamma_{av}}{(M-1)\sin^2\eta}\left(1+k-\frac{\pi}{4}L_{1/2}^2(-k)\right)}\right\}\mathrm{d}\eta}{\left(1+\frac{3N\Gamma_{av}}{(M-1)\sin^2\eta}\left(1+k-\frac{\pi}{4}L_{1/2}^2(-k)\right)\right)^{\frac{1}{2}}} \quad (54)$$

formulated as

$$P_{s,M\text{-QAM}}=\frac{4}{\pi}\left(1-\frac{1}{\sqrt{M}}\right)\frac{\sqrt{2(M-1)}}{\sqrt{6N\Gamma_{av}\left(1+k-\frac{\pi}{4}L_{1/2}^2(-k)\right)}}\times\exp\left\{\frac{-N\pi L_{1/2}^2(-k)}{8\left(1+k-\frac{\pi}{4}L_{1/2}^2(-k)\right)}\right\}-\frac{4}{\pi}\left(1-\frac{1}{\sqrt{M}}\right)^2\frac{\sqrt{\left(\sqrt{2}-1\right)(M-1)}}{\sqrt{6N\Gamma_{av}\left(1+k-\frac{\pi}{4}L_{1/2}^2(-k)\right)}}\times\exp\left\{\frac{-N\pi L_{1/2}^2\cdot(-k)}{8\left(1+k-\frac{\pi}{4}L_{1/2}^2(-k)\right)}\right\}. \quad (56)$$

Assuming a low SNR $\Gamma_{av}\ll 1$, the SEP can be simplified by approximating the first and second term of (54) as

$$1+\frac{3N\Gamma_{av}}{(M-1)\sin^2\eta}\left(1+k-\frac{\pi}{4}L_{1/2}^2(-k)\right)\approx 1\,, \quad (57)$$

and

$$\frac{\exp\left\{\frac{-\frac{3N^2\Gamma_{av}\pi}{8(M-1)\sin^2\eta}L_{1/2}^2(-k)}{1+\frac{3N\Gamma_{av}}{(M-1)\sin^2\eta}(1+k-\frac{\pi}{4}L_{1/2}^2(-k))}\right\}}{\left(1+\frac{3N\Gamma_{av}}{(M-1)\sin^2\eta}\left(1+k-\frac{\pi}{4}L_{1/2}^2(-k)\right)\right)^{\frac{1}{2}}}\approx\exp\left\{\frac{-\frac{3N^2\Gamma_{av}\pi}{8(M-1)\sin^2\eta}L_{1/2}^2(-k)}{1+\frac{3N\Gamma_{av}}{(M-1)\sin^2\eta}\left(1+k-\frac{\pi}{4}L_{1/2}^2(-k)\right)}\right\}. \quad (58)$$

Accordingly, the SEP can be simplified as follows:

$$P_{s,M\text{-QAM}}\big|_{\Gamma_{av}\ll 1}=4\left(1-\frac{1}{\sqrt{M}}\right)Q\left(\sqrt{\frac{3N^2\Gamma_{av}\pi L_{1/2}^2(-k)}{4}}\right)-\frac{4}{\pi}\left(1-\frac{1}{\sqrt{M}}\right)^2\left[\frac{\pi}{4}-\frac{N\pi L_{1/2}^2(-k)}{8\left(1+k-\frac{\pi}{4}L_{1/2}^2(-k)\right)}\times\left\{\frac{1}{(1+u)^{\frac{1}{2}}}\left(\tan^{-1}\left(\sqrt{1+u}\tan\frac{\pi}{4}\right)+\frac{\sqrt{1+u}}{2}\tan\frac{\pi}{4}\right)\right\}\right], \quad (59)$$

where u is given by

$$u=\frac{M-1}{3N\Gamma_{av}\left(1+k-\frac{\pi}{4}L_{1/2}^2(-k)\right)}. \quad (60)$$

Furthermore, (45) and (54) can be simplified if $\Gamma_{av}=0$. Specifically, the SEP can be formulated as follows:

$$P_{s,M\text{-PSK}}\big|_{\Gamma_{av}=0}=P_{s,M\text{-QAM}}\big|_{\Gamma_{av}=0}=M-1/M\,, \quad (61)$$

which is equal to $1/2$ for $M=2$.

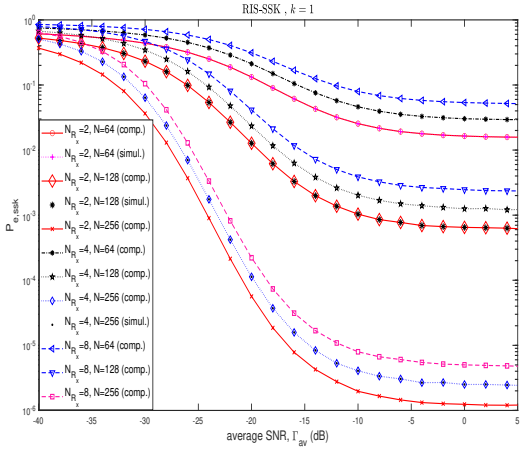

Fig. 3. $P_{e,ssk}$ versus Γ_{av} for the RIS-assisted SSK system for $k=1$, $N_{R_X}=2,4,8$, and $N=64,128,256$.

VI. Numerical Results

In this section, we validate the proposed analytical frameworks with the aid of Monte Carlo simulations. Monte Carlo results are obtained by considering 10^9 channel realizations and the analytical expressions are computed by considering a sufficient number of terms such that the relative error is less than 0.00001%.

Fig. 3 presents the PED versus the average SNR for the SSK scheme as a function of N_{R_X} and N. It is observed that the simulation and analytical results are in good agreement. Furthermore, it is observed that the $P_{e,ssk}$ decreases by increasing Γ_{av}. Additionally, the PED tends to saturate at high values of Γ_{av}, as obtained in (21). Interestingly, the $P_{e,ssk}$ is a concave function of Γ_{av} at low SNR values and is a convex function of Γ_{av} at high SNR values. Thus, there exists a value of Γ_{av} that corresponds to a point of inflection. It is also observed that the PED decreases with an increase in the value of N, and it increases with increasing the number of diversity branches. This can be attributed to the fact that a higher number of antennas at the receiver implies that the target antenna has to be chosen from a larger set which in turn increases the PED of the system.

Fig. 4 illustrates the variation of the PED with the Rician factor k. We observe that the PED degrades for larger values of the Rician factor. This can be attributed to the fact that the LoS component for the non-target antennas becomes similar to the channel of the target antenna. Moreover, for smaller values of N, the variation in the PED is minimal, i.e., the PED tends to saturate quickly.

The PED versus the average SNR for the RIS-assisted SM system with binary phase shift keying (BPSK) modulation is presented in Fig. 5. Similar to the RIS-SSK system, $P_{e,sm}$ tends to saturate at high SNR values with the saturation

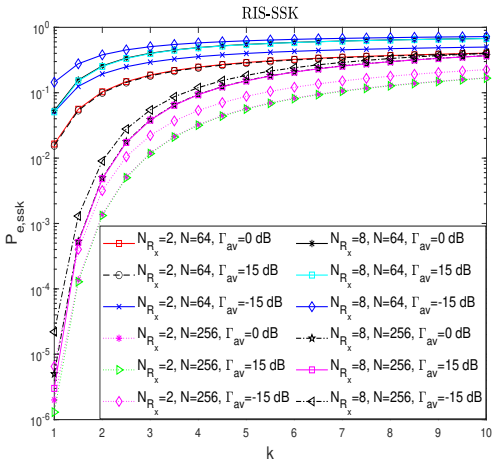

Fig. 4. $P_{e,ssk}$ versus the Rician parameter k for RIS-assisted SSK system for $N_{R_X} = 2, 8$, $N = 64, 256$, and $\Gamma_{av} = -15, 0, 15$ dB.

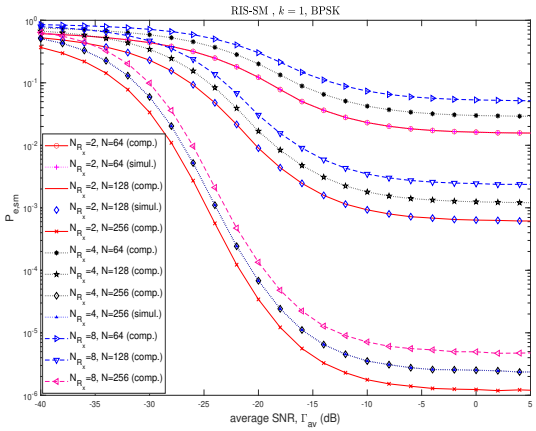

Fig. 5. $P_{e,sm}$ versus Γ_{av} for the RIS-assisted SM system with BPSK modulation for $k = 1$, $N_{R_X} = 2, 4, 8$, and $N = 64, 128, 256$.

value given in (40). Furthermore, the PED curves are concave functions of Γ_{av} at low values of the average SNR and convex functions at high values of the average SNR, indicating a point of inflection. Additionally, increasing the number of the receive antenna has a detrimental effect on the performance, while the exact opposite trend can be observed by increasing the number of reflecting elements N.

Fig. 6 illustrates the variation of the PED with the Rician parameter k for RIS-assisted SM schemes employing BPSK, 8-PSK, and 16-QAM schemes. As for the case of SSK modulation, the PED of the system tends to increase with an increasing value of the Rician factor. The degradation of the system performance is substantial for systems with higher values of N for a given N_{R_X}. Moreover, the system performance degrades by increasing the modulation order, as is evident by comparing the system performance of 8-PSK and 16-QAM with BPSK. Additionally, for a given value of N_{R_X} and N, there is little or no improvement upon increasing Γ_{av}.

The BER versus the average SNR for the SSK scheme and the SM scheme with QPSK and 8-PSK modulation with $m = 2$ presented in Fig. 7. Additionally, the BER curves are obtained by using the union-bound as follows:

$$P_{b,ssk} \leq N_{R_X} P_{e,ssk}/2\,, \tag{62a}$$

$$P_{b,sm} \approx \frac{\left(1-\left(N_{R_X}-1\right)P_{e,sm}\right)P_{s,M\text{-QAM}/M\text{-PSK}}}{\log_2\left(NN_{R_X}\right)} + \frac{\left(N_{R_X}-1\right)P_{e,M\text{-QAM}/M\text{-PSK}}}{2}\,, \tag{62b}$$

where $P_{e,ssk}$ and $P_{e,sm}$ are obtained from (21) and (32), respectively. We see that the performance of the RIS-assisted SSK modulation scheme is outperformed by the QPSK and 8-PSK modulation schemes. It is noted that the performance of the QPSK scheme is comparatively better than that of the 8-PSK scheme.

VII. Conclusions

In this work, we studied an RIS-assisted receive diversity wireless communication system where the transmitter utilizes IM-based schemes for data transmission, and the receiver employs a greedy detection scheme to select the receiver antenna with the maximum received energy for demodulation. The RIS is part of the transmitter and utilizes SSK or M-ary QAM/M-PSK-based SM schemes for data modulation. Further, the envelopes of the channel gains between the RIS elements and the receiver are assumed to follow a Rician distribution. An analytical framework based on a c.f. approach was presented to derive closed-form expressions of the PED and SEP. Furthermore, asymptotic expressions of the PED and BER at low and high SNRs reveal the presence of a point of inflection with respect to the average SNR. Numerical results were illustrated to validate the proposed analytical frameworks.

Appendix I
Derivation of (17)

The PPED in (12) can be expressed as

$$\begin{aligned}\Pr\left\{X_{ssk} < Y_{ssk}\right\} &= 1 - \int_0^\infty F_{Y_{ssk}}\left(x\right) f_{X_{ssk}}\left(x\right) \mathrm{d}x \\ &= 1 - \int_0^\infty \int_0^x \frac{\exp\left\{-\frac{y+E_s N^2|\mu|^2}{N\sigma_h^2 E_s + N_0}\right\}}{N\sigma_h^2 E_s + N_0} \\ &\quad \times I_0\left(\frac{2\sqrt{E_s N^2|\mu|^2 y}}{N\sigma_h^2 E_s + N_0}\right) f_{X_{ssk}}\left(x\right) \mathrm{d}y\mathrm{d}x,\end{aligned} \tag{63}$$

where $F_{X_{ssk}}\left(\cdot\right)$ and $f_{X_{ssk}}\left(\cdot\right)$ denote the cumulative distribution function (c.d.f.) and the probability density function (p.d.f.) of X_{ssk}, respectively, and $I_0(\cdot)$ denotes the modified Bessel function of the zeroth order and the first kind.

Utilizing the series-form expansions of $I_0(x)$ and $\exp\left\{x\right\}$ as

$$I_0(x) = \sum_{\ell=0}^{\infty} \frac{\left(\frac{x^2}{4}\right)^\ell}{\left(\ell!\right)^2} \quad , \quad \exp\left\{x\right\} = \sum_{p=0}^{\infty} \frac{x^p}{p!}\,, \tag{64}$$

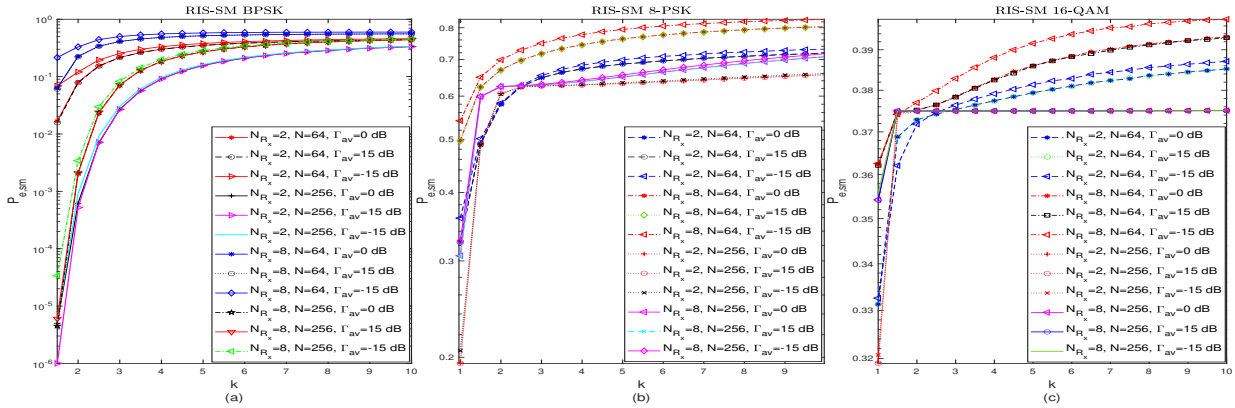

Fig. 6. $P_{e,sm}$ versus the Rician parameter k for $N_{R_X} = 2, 8$, $N = 64, 256$, and $\Gamma_{av} = -15, 0, 15$ dB for (a) BPSK; (b) 8-PSK; and (c) 16-QAM constellations for the RIS-assisted SM wireless system.

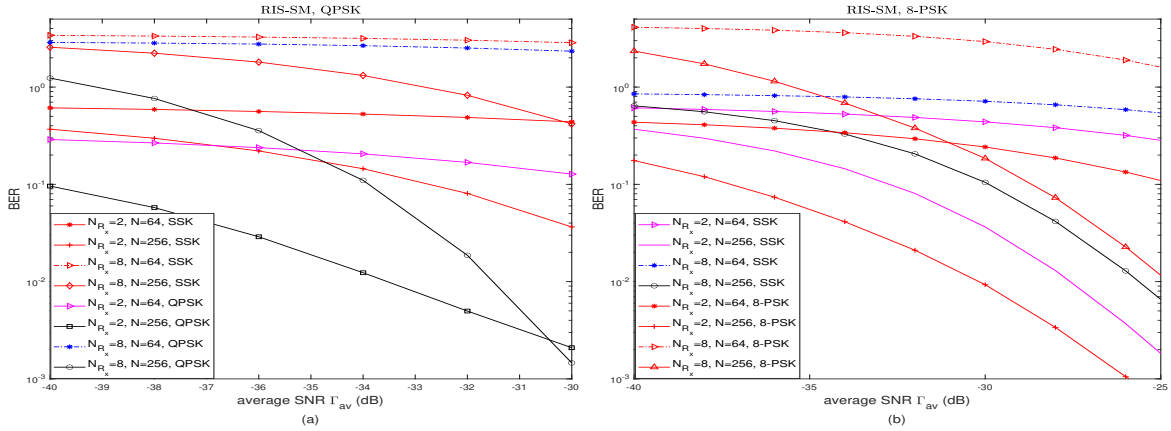

Fig. 7. BER versus Γ_{av} for RIS-assisted SSK and SM systems with (a) QPSK and (b) 8-PSK modulation schemes for $k = 1$, $N_{R_X} = 2, 8$, and $N = 64, 256$.

in (63), $\Pr\{X_{ssk} < Y_{ssk}\}$ is obtained as

$$\begin{aligned}
&\Pr\{X_{ssk} < Y_{ssk}\} \\
&= 1 - \sum_{\ell=0}^{\infty}\sum_{p=0}^{\infty} \frac{(-1)^p \left(E_s N^2 |\mu|^2\right)^\ell}{\left(N\sigma_h^2 E_s + N_0\right)^{2\ell+p+1} (\ell!)^2 (p!)} \\
&\quad \times \exp\left\{-\frac{E_s N^2 |\mu|^2}{N\sigma_h^2 E_s + N_0}\right\} \int_0^\infty \left[\int_0^x y^{\ell+p} \mathrm{d}y\right] f_{X_{ssk}}(x)\,\mathrm{d}x \\
&= 1 - \sum_{\ell=0}^{\infty}\sum_{p=0}^{\infty} \frac{(-1)^p \left(E_s N^2 |\mu|^2\right)^\ell}{\left(N\sigma_h^2 E_s + N_0\right)^{2\ell+p+1} (\ell!)^2\, p!\, (\ell+p+1)} \\
&\quad \times \exp\left\{-\frac{E_s N^2 |\mu|^2}{N\sigma_h^2 E_s + N_0}\right\} \int_0^\infty x^{\ell+p+1} f_{X_{ssk}}(x)\,\mathrm{d}x.
\end{aligned} \tag{65}$$

It can be observed from (65) that the integral $\int_0^\infty x^{\ell+p+1} f_{X_{ssk}}(x)\,\mathrm{d}x$ can be computed by using the c.f. of X_{ssk} as

$$\begin{aligned}
\int_0^\infty x^{\ell+p+1} f_{X_{ssk}}(x)\,\mathrm{d}x &= \mathbf{E}\left[X_{ssk}^{\ell+p+1}\right] \\
&= \frac{1}{\jmath^{\ell+p+1}} \left[\frac{\partial^{\ell+p+1}}{\partial\omega^{\ell+p+1}} \Psi_{X_{ssk}}(\jmath\omega)\right]\Big|_{\omega=0},
\end{aligned} \tag{66}$$

where the expression of $\Psi_{X_{ssk}}(\jmath\omega)$ is given in (16). Moreover, it can be observed from (66) that the solution of the integral requires the $(\ell+p+1)$-th derivative of the c.f. of X_{ssk}. However, from the structure of the c.f. in (16), a direct differentiation of $\Psi_{X_{ssk}}(\jmath\omega)$ would be mathematically intractable. Thus, we employ the Faa di Bruno's formula to compute the derivatives as

$$\begin{aligned}
\frac{\partial^{\ell+p+1}}{\partial\omega^{\ell+p+1}} \Psi_{X_{ssk}}(\jmath\omega) &= (\ell+p+1)!\, \Psi_{X_{ssk}}(\jmath\omega) \\
&\times \sum_{\substack{q_1,\ldots,q_{\ell+p+1} \\ 0\le q_1,\ldots,q_{\ell+p+1}\le \ell+p+1 \\ q_1+2q_2+\ldots+(\ell+p+1)q_{\ell+p+1}=\ell+p+1}} \prod_{r=1}^{\ell+p+1} \frac{1}{q_r!} \left(\frac{H_{ssk}^r(\jmath\omega)}{r!}\right)^{q_r},
\end{aligned} \tag{67}$$

where the summation over the set $S_{q,\ell+p+1}$ is carried out for all the possible tuples of $q_1,\ldots,q_{\ell+p+1}$ such that $\sum_{r=1}^{\ell+p+1} r q_r = \ell+p+1$. Moreover, $H_{ssk}^r(\jmath\omega)$ denotes the r-th derivative of the function $H_{ssk}(\jmath\omega)$ defined as

$$\begin{aligned}
H_{ssk}(\jmath\omega) \triangleq \ln \Psi_{X_{ssk}}(\jmath\omega) &= \frac{\jmath\omega\mu_X^2}{1-2\jmath\omega(b+c)} - \frac{1}{2}\ln(1-2\jmath\omega c) \\
&- -\frac{1}{2}\ln(1-2\jmath\omega(b+c)).
\end{aligned} \tag{68}$$

Using (68), $H_{ssk}^{r}\left(\jmath\omega\right)$ can be written as

$$H_{ssk}^{r}\left(\jmath\omega\right)=\frac{\jmath r!\mu_X^2\left(2\jmath\left(b+c\right)\right)^{r-1}}{\left(1-2\jmath\omega\left(b+c\right)\right)^{r}}+\frac{\jmath r!\omega\mu_X^2\left(2\jmath\left(b+c\right)\right)^{r}}{\left(1-2\jmath\omega\left(b+c\right)\right)^{r+1}}+\frac{\left(r-1\right)!\left(2\jmath\left(b+c\right)\right)^{r}}{2\left(1-2\jmath\omega\left(b+c\right)\right)^{r}}+\frac{\left(r-1\right)!\left(2\jmath c\right)^{r}}{2\left(1-2\jmath\omega c\right)^{r}}. \quad (69)$$

Further, from (66), we need to evaluate the derivative at $\omega=0$, implying that

$$H_{ssk}^{r}(\jmath\omega)\Big|_{\omega=0}=\frac{\jmath^r\left(r-1\right)!}{2^{1-r}}\left[r\mu_X^2\left(b+c\right)^{r-1}+\left(b+c\right)^{r}+c^{r}\right],$$
$$\Psi_{X_{ssk}}(\jmath\omega)\Big|_{\omega=0}=1, \quad (70)$$

where the variables μ_X, b, and c are given in (15). Substituting (70) in (66) and substituting the result in (16), we obtain the series expression of $\Pr\left\{X_{ssk}<Y_{ssk}\right\}$ in (17). This completes the proof of Theorem I. ■

Appendix II
Derivation of (35)

Proceeding along the same lines as for the RIS-assisted SSK scheme, the PPED from (28) is obtained as

$$\begin{aligned}\Pr\left\{X_{sm}<Y_{sm}\right\}&=1-\int_0^{\infty}F_{Y_{sm}}\left(y\right)f_{X_{sm}}\left(x\right)\mathrm{d}x\\&=1-\int_0^{\infty}\int_0^{x}\frac{\exp\left\{-\frac{y+E_sN^2|\mu|^2|}{N\sigma_h^2E_s+N_0}\right\}}{N\sigma_hE_s+N_0}\\&\times I_0\left(\frac{2\sqrt{E_sN^2|\mu|^2|y}}{N\sigma_h^2E_s+N_0}\right)f_{X_{sm}}\left(x\right)\mathrm{d}y\mathrm{d}x. \quad (71)\end{aligned}$$

Simplifying (71) by using the series expansion of the modified Bessel function of the zeroth order and the first kind and the exponential function in (64), the expression in (71) can be further simplified as

$$\begin{aligned}&\Pr\left\{X_{sm}<Y_{sm}\right\}\\&=1-\sum_{\ell=0}^{\infty}\sum_{p=0}^{\infty}\frac{\left(-1\right)^p\left(E_sN^2\left|\mu\right|^2\right)^{\ell}}{\left(N\sigma_h^2E_s+N_0\right)^{2\ell+p+1}\left(\ell!\right)^2\left(p!\right)}\\&\times\exp\left\{-\frac{E_sN^2\left|\mu\right|^2}{N\sigma_h^2E_s+N_0}\right\}\int_0^{\infty}\left[\int_0^{x}y^{\ell+p}\mathrm{d}y\right]f_{X_{sm}}\left(x\right)\mathrm{d}x\\&=1-\sum_{\ell=0}^{\infty}\sum_{p=0}^{\infty}\frac{\left(-1\right)^p\left(E_sN^2\left|\mu\right|^2\right)^{\ell}}{\left(N\sigma_h^2E_s+N_0\right)^{2\ell+p+1}\left(\ell!\right)^2p!\left(\ell+p+1\right)}\\&\times\exp\left\{-\frac{E_sN^2\left|\mu\right|^2}{N\sigma_h^2E_s+N_0}\right\}\int_0^{\infty}x^{\ell+p+1}f_{X_{sm}}\left(x\right)\mathrm{d}x.\\&. \quad (72)\end{aligned}$$

The integral in (72) can be solved by using the c.f. of X_{sm} as

$$\begin{aligned}\int_0^{\infty}x^{\ell+p+1}f_{X_{sm}}\left(x\right)\mathrm{d}x&=\mathbf{E}\left[X_{sm}^{\ell+p+1}\right]\\&=\frac{1}{\jmath^{\ell+p+1}}\left[\frac{\partial^{\ell+p+1}}{\partial\omega^{\ell+p+1}}\Psi_{X_{sm}}\left(\jmath\omega\right)\right]\Big|_{\omega=0}, \quad (73)\end{aligned}$$

where, using Faa di Bruno's formula, we have

$$\begin{aligned}\frac{\partial^{\ell+p+1}}{\partial\omega^{\ell+p+1}}\Psi_{X_{sm}}\left(\jmath\omega\right)&=\left(\ell+p+1\right)!\,\Psi_{X_{sm}}\left(\jmath\omega\right)\\&\times\sum_{\substack{q_1,\ldots,q_{\ell+p+1}\\0\le q_1,\ldots,q_{\ell+p+1}\le\ell+p+1\\q_1+2q_2+\ldots+(\ell+p+1)q_{\ell+p+1}=\ell+p+1}}\prod_{r=1}^{\ell+p+1}\frac{1}{q_r!}\left(\frac{H_{sm}^{r}\left(\jmath\omega\right)}{r!}\right)^{q_r}. \quad (74)\end{aligned}$$

Thus, we need to compute the r-th derivative of $H_{sm}\left(\jmath\omega\right)$ defined as

$$\begin{aligned}H_{sm}\left(\jmath\omega\right)\triangleq\ln\Psi_{X_{sm}}\left(\jmath\omega\right)=&\frac{\jmath\omega\mu_1^2}{1-2\jmath\omega\left(b_1+c\right)}+\frac{\jmath\omega\mu_2^2}{1-2\jmath\omega\left(b_2+c\right)}\\&-\frac{1}{2}\ln\left(1-2\jmath\omega(b_2+c)\right)-\frac{1}{2}\ln\left(1-2\jmath\omega\left(b_1+c\right)\right), \quad (75)\end{aligned}$$

which can be obtained by simple algebraic manipulations as

$$\begin{aligned}H_{sm}^{r}\left(\jmath\omega\right)&=\frac{\jmath r!\omega\mu_1^2\left(2\jmath\left(b_1+c\right)\right)^{r-1}}{\left(1-2\jmath\omega\left(b_1+c\right)\right)^{r+1}}+\frac{\jmath r!\omega\mu_2^2\left(2\jmath\left(b_2+c\right)\right)^{r-1}}{\left(1-2\jmath\omega\left(b_2+c\right)\right)^{r+1}}\\&+\frac{\jmath r!\omega\mu_1^2\left(2\jmath\left(b_1+c\right)\right)^{r}}{\left(1-2\jmath\omega\left(b_1+c\right)\right)^{r+1}}+\frac{\jmath r!\omega\mu_2\left(2\jmath\left(b_2+c\right)\right)^{r}}{\left(1-2\jmath\omega\left(b_2+c\right)\right)^{r+1}}\\&+\frac{\left(r-1\right)!\left(2\jmath\left(b_1+c\right)\right)^{r}}{2\left(1-2\jmath\omega\left(b_1+c\right)\right)^{r}}+\frac{\left(r-1\right)!\left(2\jmath(b_2+c)\right)^{r}}{2\left(1-2\jmath\omega(b_2+c)\right)^{r}}. \quad (76)\end{aligned}$$

To compute the PPED, we require the values of the derivatives at $\omega=0$, which are obtained as

$$\begin{aligned}H_{sm}^{r}(\jmath\omega)\Big|_{\omega=0}=&\jmath^r\left(r-1\right)!2^{r-1}\left[r\mu_1^2\left(b_1+c\right)^{r-1}+r\mu_2^2\left(b_2+c\right)^{r-1}\right.\\&\left.+\left(b_1+c\right)^{r}+\left(b_2+c\right)^{r}\right]\\\Psi_{X_{sm}}(\jmath\omega)\Big|_{\omega=0}=&\,1. \quad (77)\end{aligned}$$

Substituting the results in (73)-(77), we obtain (35). This completes the proof of Theorem II. ■

References

[1] S. Yrjölä, P. Ahokangas, and M. Matinmikko-Blue, "Value creation and capture from technology innovation in the 6G era," *IEEE Access*, vol. 10, pp. 16299–16319, 2022.

[2] Z. Zhang et al., "6G wireless networks: Vision requirements architecture and key technologies," *IEEE Veh. Technol. Mag.*, vol. 14, no. 3, pp. 28-41, Sep. 2019.

[3] W. Saad, M. Bennis and M. Chen, "A vision of 6G wireless systems: Applications trends technologies and open research problems," *IEEE Netw.*, vol. 34, no. 3, pp. 134-142, May/Jun. 2020.

[4] A. Kaushik and M. Z. Shakir, "Non-terrestrial networks: Have we found that ultimate catalyst for global connectivity in 6G?," *IEEE ComSoc Technology News* (CTN), Dec. 2022.

[5] A. Kaushik, E. Vlachos, C. Tsinos, J. Thompson, and S. Chatzinotas, "Joint bit allocation and hybrid beamforming optimization for energy efficient millimeter wave MIMO Systems," *IEEE Trans. Green Commun. Netw.*, vol. 5, no. 1, pp. 119-132, Mar. 2021.

[6] X. Gao, R. Liu, A. Kaushik, and H. Zhang, "Dynamic resource allocation for virtual network function placement in satellite edge clouds," *IEEE Trans. Netw. Sci. Eng.*, vol. 9, no. 4, pp. 2252-2265, Jul.-Aug. 2022.

[7] C. H. Lin et al., "Automatic inverse design of high-performance beam-steering metasurfaces via genetic-type tree optimization," *Nano Lett.*, pp. 4981–4989, Jun. 2021.

[8] Y. Han, S. Zhang, L. Duan, and R. Zhang, "Cooperative double-IRS aided communication: Beamforming design and power scaling," *IEEE Wireless Commun. Lett.*, vol. 9, no. 8, pp 1206–1210, Aug. 2020.

[9] W. Ni, Y. Liu, Y. C. Eldar, Z. Yang, and H. Tian, "STAR-RIS integrated nonorthogonal multiple access and over-the-air federated learning: framework, analysis, and optimization," *IEEE Internet Things J.*, vol. 9, no. 18, pp. 17136-17156, Sep. 2022.

[10] S. P. Dash, S. Joshi, and S. Aïssa, "Envelope distribution of two correlated complex Gaussian random variables and application to the performance evaluation of RIS-assisted communications," *IEEE Commun. Lett.*, vol. 26, no. 9, pp. 2018–2022, Sep. 2022.

[11] Q. Li, M. Wen, and M. Di Renzo, "Single-RF MIMO: From spatial modulation to metasurface-based modulation," *IEEE Wireless Commun.*, vol. 28, pp. 88–95, Aug. 2021.

[12] A. K. Padhan, H. K. Sahu, P. R. Sahu, and S. R. Samantaray, "RIS assisted dual-hop mixed PLC/RF for smart grid applications," *IEEE Commun. Lett.*, vol. 25, no. 11, pp. 3523–3527, Nov. 2021.

[13] Y. Wang, W. Zhang, Y. Chen, C. -X. Wang, and J. Sun, "Novel multiple RIS-assisted communication for 6G networks," *IEEE Commun. Lett.*, vol. 26, no. 6, pp. 1413–1417, Jun. 2022.

[14] M. Di Renzo et al., "Reconfigurable intelligent surfaces vs. relaying: Differences, similarities, and performance comparison," *IEEE Open J. Commun. Soc.*, vol. 1, pp. 798–807, 2020.

[15] M. Di Renzo, F. H. Danufane, and S. Tretyakov, "Communication models for reconfigurable intelligent surfaces: From surface electromagnetics to wireless networks optimization," *Proc. IEEE*, vol. 110, no. 9, pp. 1164-1209, Sep. 2022.

[16] Q. Cheng et al., "Reconfigurable intelligent surfaces: Simplified-architecture transmitters—from theory to implementations," *Proc. IEEE*, vol. 110, no. 9, pp. 1266-1289, Sep. 2022.

[17] S. P. Dash, R. K. Mallik, and N. Pandey, "Performance analysis of an index modulation-based receive diversity RIS-assisted wireless communication system," *IEEE Commun. Lett.*, vol. 26, no. 4, pp. 768–772, Apr. 2022.

[18] E. Basar, "Reconfigurable intelligent surface-based index modulation: A new beyond MIMO paradigm for 6G," *IEEE Trans. Commun.*, vol. 68, no. 5, pp. 3187–3196, May 2020.

[19] A. P. Ajayan, S.P. Dash, and B. Ramkumar, "Performance analysis of an IRS-aided wireless communication system with spatially correlated channels," *IEEE Commun. Lett.*, vol. 11, no. 3, pp 563–567, Mar. 2022.

[20] E. Basar, "Transmission through large intelligent surfaces: A new frontier in wireless communication," in *Proc. Euro. Conf. Netw Commun. (EuCNC)*, Valencia, Spain Jun. 2019, pp 112–117.

[21] X. Tan, Z. Sun, J. M. Jornet, and D. Pados, "Increasing indoor spectrum sharing capacity using smart reflect-array," in *Proc. IEEE Int. Conf. Commun. (ICC)*, Kuala Lumpur, Malaysia, May 2016, pp. 1–6.

[22] Q. Li, M. Wen, L. Xu, and K. Li, "Reconfigurable intelligent surface-aided number modulation for symbiotic active/passive transmission," *IEEE Internet Things J.*, Early Access, pp. 1–12, Nov. 2022.

[23] X. Gan, C. Zhong, C. Huang, and Z. Zhang, "RIS-assisted multi-user MISO communications exploiting statistical CSI," *IEEE Trans. Commun.*, vol. 69, no. 10, pp. 6781–6792, Oct. 2021.

[24] X. Gan, C. Zhong, C. Huang, Z. Yang, and Z. Zhang, "Multiple RISs assisted cell-free networks with two-timescale CSI: Performance analysis and system design," *IEEE Trans. Commun.*, vol. 70, no. 11, pp. 7696–7710, Nov. 2022.

[25] C. Huang et al., "Multi-hop RIS-empowered terahertz communications: A DRL-based hybrid beamforming design," *IEEE J. Sel. Areas Commun.*, vol. 39, no. 6, pp. 1663–1677, Jun. 2021.

[26] S. Chen, A. Kaushik, and C. Masouros, "Pre-scaling and codebook design for joint radar and communication based on index modulation," in *Proc. IEEE Glob. Commun. Conf. (GLOBECOM)*, Rio de Janerio, Brazil, pp. 1-5, Dec. 2022.

[27] T. Huang, N. Shlezinger, X. Xu, Y. Liu and, Y. C. Eldar, "MAJoRCom: A dual-function radar communication system using index modulation," *IEEE Trans. Signal Process.*, vol. 68, pp. 3423-3438, 2020.

[28] X. Cheng, M. Zhang, M. Wen, and L. Yang, "Index modulation for 5G: Striving to do more with less," *IEEE Wireless Commun.*, vol 25, no. 2, pp. 126–132, Apr. 2018.

[29] J. Jeganathan, A. Ghrayeb, L. Szczecinski, and A. Ceron, "Space shift keying modulation for MIMO channels," *IEEE Trans. Wireless Commun.*, vol. 8, no. 7, pp. 3692–3703, Jul. 2009.

[30] M. Di Renzo and H. Haas, "Improving the performance of space shift keying (SSK) modulation via opportunistic power allocation," *IEEE Commun. Lett.*, vol. 14, no. 6, pp. 500–502, Jun. 2010.

[31] S. S. Ikki and R. Mesleh, "A general framework for performance analysis of space shift keying (SSK) modulation in the presence of Gaussian imperfect estimations," *IEEE Commun. Lett.*, vol. 16, no. 2, pp. 228–230, Feb. 2012.

[32] A. Bouhlel, M. M. Alsmadi, E. Saleh, S. Ikki, and A. Sakly, "Performance analysis of RIS-SSK in the presence of hardware impairments," in *Proc. IEEE Per. Indoor Mobile Radio Commun. (PIMRC)*, Sep. 2021, pp. 537–542.

[33] M. Di Renzo and H. Haas, "A general framework for performance analysis of space shift keying (SSK) modulation for MISO correlated Nakagami-m fading channels," *IEEE Trans. Commun.*, vol. 58, no. 9, pp. 2590-2603, Sep. 2010.

[34] Q. Li, M. Wen, S. Wang, G. C. Alexandropoulos, and Y. C. Wu, "Space shift keying with reconfigurable intelligent surfaces: Phase configuration designs and performance analysis," *IEEE Open J. Commun. Soc.*, vol. 2, pp. 322–333, Feb. 2021.

[35] K. Asmoro and S. Y. Shin, "RIS grouping based index modulation for 6G telecommunications," *IEEE Wireless Commun.*, vol. 11, no. 11, pp. 2410–2414, Nov. 2022.

[36] S. Guo, S. Lv, H. Zhang, J. Ye, and P. Zhang, "Reflecting modulations," *IEEE J. Sel. Area Commun.*, vol 38, no. 11, pp. 2548–2561, Nov. 2020.

[37] J. Yuan, M. Wen, Q. Li, E. Basar, G. C. Alexandropoulos, and G. Chen, "Receive quadrature reflecting modulation for RIS-empowered wireless communications," *IEEE Trans. Veh. Technol.*, vol. 70, no. 5, pp. 5121-5125, May 2021.

[38] M. Di Renzo and H. Haas, "Space shift keying (SSK) modulation with partial channel state information: Optimal detector and performance analysis over fading channels," *IEEE Trans. Commun.*, vol. 58, no. 11, pp. 3196–3210, Nov. 2010.

[39] A. M. Salhab and M. H. Samuh, "Accurate performance analysis of reconfigurable intelligent surfaces over Rician fading channels," *IEEE Wireless Commun.*, vol. 10, no. 5, pp. 1051-1055, May 2021.

[40] C. Singh, C. H. Lin, and K. Singh, "Capacity and performance analysis of RIS assisted communication over Rician fading channels," Nov 2021, *arXiv:2111.04783v1*. [online]. Available: https://arxiv.org/abs/2111.04783v1.

[41] K. Xu, J. Zhang, X. Yang, S. Ma, and G. Yang, "On the sum-rate of RIS-assisted MIMO multiple-access channels over spatially correlated Rician fading," *IEEE Trans. Commun.*, vol. 69, no. 12, pp. 8228-8241, Dec. 2021.

[42] M. Simon and M. S. Alouini, *Digital Communications Over Fading Channels*, 2nd ed. Hoboken, NJ, USA: Wiley, 2005.

Aritra Basu received his B.Tech. degree in electronics and communication engineering from Heritage Institute of Technology, Kolkata, India, in 2021. He pursued his M.Tech. degree in electronics and communication engineering from the Indian Institute of Technology (IIT) Bhubaneswar, India, in 2023. He is currently working towards a Ph.D. degree at the Institut National de la Recherche Scientifique, Montreal, QC, Canada. His research focuses on reconfigurable intelligent surfaces, channel modeling, and sustainable communication systems.

Soumya P. Dash (Member) is with the faculty of the School of Electrical Sciences, IIT Bhubaneswar, where he is currently an Assistant Professor. His research interests include communication theory for hybrid communication systems, power line communications, smart grid communications, next-generation wireless communication systems, reconfigurable intelligent surfaces, quantum communications, visible light communications, and diversity combining. He is a Member of the IEEE Communications and Vehicular Technology Societies. He is a Young Associate of the Indian National Academy of Engineering (INAE) and is the recipient of the Odisha Young Scientist Award, VDGOOD Young Scientist Award, and the President of India Gold Medal for the academic year 2013-14 for obtaining the highest CGPA amongst the students graduating with B.Tech. (H) degree from IIT Bhubaneswar.

Aryan Kaushik (Member) is Assistant Professor with University of Sussex, UK, since 2021. Previously he has been with University College London, University of Edinburgh, Hong Kong University of Science and Technology, and held visiting appointments at Imperial College London, University of Luxembourg, Athena RC, and Beihang University. He is Editor of two books, IEEE CTN, IEEE OJCOMS (Best Editor Award 2023), IEEE COMML (Exemplary Editor 2023) and several IEEE special issues. He has delivered over 45 invited speeches/tutorials globally, and been involved in over 6 Organizing/Technical Program Committees of flagship IEEE conferences such as IEEE ICC 2024-26.

Debasish Ghose (Senior Member) received Ph.D. degree in Information and Communication Technology from the University of Agder, Grimstad, Norway in 2019. He did his post-doc at the same university from 2021 to 2022. Prior to his post-doc, he worked as a system developer at Confirmit, Grimstad, Norway from 2020 to 2021. Currently, he is with the School of Economics, Innovation, and Technology, Kristiania University College, Bergen, Norway as Associate Professor. His research interests include protocol design, modeling, and performance evaluation of the Internet of things. His other research interests include edge and fog computing, data analytics, cyber security, and machine learning.

Marco Di Renzo (Fellow, IEEE) is a CNRS Research Director (Professor) and the Head of the Intelligent Physical Communications group in the Laboratory of Signals and Systems at Paris-Saclay University – CNRS and CentraleSupelec, Paris, France. He is a Fellow of the IEEE, IET, AAIA; an Ordinary Member of the European Academy of Sciences and Arts, an Ordinary Member of the Academia Europaea; a Highly Cited Researcher. He holds the 2023 France-Nokia Chair of Excellence in ICT. He served as the Editor-in-Chief of IEEE Communications Letters in 2019-2023 and he is now serving in the Advisory Board. In 2024-2025, he will be serving as a Voting Member of the Fellow Evaluation Standing Committee and as the Director of Journals of the IEEE Communications Society. He is also a Vice-Chair and a Rapporteur of ETSI ISG RIS.

Yonina C. Eldar (S'98–M'02–SM'07-F'12) received the B.Sc. degree in Physics in 1995 and the B.Sc. degree in Electrical Engineering in 1996 both from Tel-Aviv University (TAU), Tel-Aviv, Israel, and the Ph.D. degree in Electrical Engineering and Computer Science in 2002 from the Massachusetts Institute of Technology (MIT), Cambridge. She is currently a Professor in the Department of Mathematics and Computer Science, Weizmann Institute of Science, Rehovot, Israel where she holds the Dorothy and Patrick Gorman Professorial Chair and heads the Center for Biomedical Engineering. She was previously a Professor in the Department of Electrical Engineering at the Technion, where she held the Edwards Chair in Engineering. She is a member of the Israel Academy of Sciences and Humanities and of the Academia Europaea (elected 2023), an IEEE Fellow, a EURASIP Fellow, a Fellow of the Asia-Pacific Artificial Intelligence Association, and a Fellow of the 8400 Health Network. Her research interests are in the broad areas of statistical signal processing, sampling theory and compressed sensing, learning and optimization methods, and their applications to biology, medical imaging and optics.